32-S-2R

Duplicate

CRREL REPORT 77-17

Ice accumulation on ocean structures

32-621

Cover: U.S. Coast Guard Cutter Staten Island *in Bering Sea in 1969. (Photograph by L. David Minsk.)*

CRREL Report 77-17

Ice accumulation on ocean structures

L. David Minsk

August 1977

Prepared for
MARATHON OIL COMPANY
By
CORPS OF ENGINEERS, U.S. ARMY
COLD REGIONS RESEARCH AND ENGINEERING LABORATORY
HANOVER, NEW HAMPSHIRE

REPORT DOCUMENTATION PAGE

READ INSTRUCTIONS BEFORE COMPLETING FORM

1. REPORT NUMBER: CRREL Report 77-17	2. GOVT ACCESSION NO.
3. RECIPIENT'S CATALOG NUMBER	
4. TITLE (and Subtitle): ICE ACCUMULATION ON OCEAN STRUCTURES	5. TYPE OF REPORT & PERIOD COVERED
	6. PERFORMING ORG. REPORT NUMBER
7. AUTHOR(s): L. David Minsk	8. CONTRACT OR GRANT NUMBER(s): Reimbursable Project Order No. TJC
9. PERFORMING ORGANIZATION NAME AND ADDRESS: U.S. Army Cold Regions Research and Engineering Laboratory, Hanover, New Hampshire 03755	10. PROGRAM ELEMENT, PROJECT, TASK AREA & WORK UNIT NUMBERS
11. CONTROLLING OFFICE NAME AND ADDRESS: U.S. Army Cold Regions Research and Engineering Laboratory, Hanover, New Hampshire 03755	12. REPORT DATE: August 1977
	13. NUMBER OF PAGES: 46
14. MONITORING AGENCY NAME & ADDRESS (if different from Controlling Office)	15. SECURITY CLASS. (of this report): Unclassified
	15a. DECLASSIFICATION/DOWNGRADING SCHEDULE

16. DISTRIBUTION STATEMENT (of this Report)

Approved for public release; distribution unlimited.

17. DISTRIBUTION STATEMENT (of the abstract entered in Block 20, if different from Report)

18. SUPPLEMENTARY NOTES

19. KEY WORDS (Continue on reverse side if necessary and identify by block number)

Cold regions
Deicing systems
Ice
Ice formation indicators
Ice prevention
Oceans
Ships

20. ABSTRACT (Continue on reverse side if necessary and identify by block number)

A literature search was made for information on the accretion of ice on ocean structures and on methods for control. The bulk of the reports were in Russian, with some additional Japanese, British, American, Canadian, and Icelandic sources. Analysis of icing reports indicated that sea spray is the most important cause of ship icing, with lesser amounts due to freezing rain, snow, and fog. Icing is a potential danger whenever air temperatures are below the freezing point of water and the sea temperature is 6°C or lower. Theoretical work on the ice accretion process is discussed, and a method is suggested, based on Russian experiments, for calculating the sea spray accumulation rate for cylindrical and flat surfaces as a function of water source temperature, air temperature, and wind speed. Other factors that influence icing severity are ship size and configuration, angle between ship course and water heading,

20. Abstract (cont'd)

and ship speed. Icing in the north temperate latitudes generally occurs in the rear of barometric depressions. Maps showing limits of various degrees of icing severity are included. Atmospheric icing measurements on tall land-based structures are presented, and potential maximum accumulations estimated. Control measures are discussed, though no completely effective method is available. Mechanical (impaction) methods are the most common, but experiments have been conducted on heated, icephobic, and deformable surfaces, and with freezing point depressants. No device for the unequivocal measurement of ice accumulation is available, though some experimental methods are suitable for controlled testing; it is recommended that a device be developed.

PREFACE

This report was prepared by L. David Minsk, Research Physical Scientist, of the Applied Research Branch, Experimental Engineering Division, U.S. Army Cold Regions Research and Engineering Laboratory. It was funded by the Marathon Oil Company under Reimbursable Project Order No. TJC, *For Superstructure Icing Study.*

Dr. Andrew Assur, James Wuebben, and Stephen Ackley of CRREL technically reviewed the manuscript.

The author wishes to thank Dr. Kazuhiko Itagaki of CRREL for his assistance in searching the Japanese literature and in providing translations of portions of selected reports, and Dr. George Swinzow, also of CRREL, for his assistance in translating portions of the Russian literature.

CONTENTS

ILLUSTRATIONS

TABLES

CONVERSION FACTORS: U.S. CUSTOMARY TO METRIC (SI) UNITS OF MEASUREMENT

These conversion factors include all the significant digits given in the conversion tables in the ASTM *Metric Practice Guide* (E 380), which has been approved for use by the Department of Defense. Converted values should be rounded to have the same precision as the original (see E 380).

Multiply	*By*	*To obtain*
foot	3.048*	meter
ton	907.1847	kilogram
knot	0.5144444	meter/second
mile	1.6093	kilometer

* Exact

ICE ACCUMULATION ON OCEAN STRUCTURES

L. David Minsk

INTRODUCTION

An extensive search of references from Russian, Japanese, British, American, Canadian, and Icelandic sources was made for material pertaining to the mechanism, extent, and frequency of icing of sea structures, the conditions conducive to icing incidence, and methods for control. Most references found discuss only ice on ships, since this is the most serious hazard to an extensive economic activity. Many of these references are further limited to a discussion of the effects of the ice burden on stability.

Ship icing research is relatively recent. It received its initial stimulus when the British Shipbuilding Research Association sponsored coldroom model tests in 1955 (*Polar Record* 1958), following the loss of the British trawlers *Lorella* and *Roderigo*. Increased fishing activity in northern waters, and the increasing loss of trawlers from ice accretion, has led a number of other countries to investigate the problem, and to attempt to forecast ice accumulation conditions and their severity. The German fishing industry, for example, has been provided with meteorological ships in their fishing grounds (Mertins 1968). In 1969 the Intergovernmental Maritime Consultative Organization (IMCO), headquartered in London, established a Subcommittee on Safety of Fishing Vessels, which has served as a central clearing house for ship icing reports from world-wide fishing fleets. The Commission for Marine Meteorology (CMM) of the World Meteorological Organization (WMO) has cooperated with IMCO in studying the meteorological aspects of ship icing, and the most recent and comprehensive review of this problem has been prepared by the Rapporteur of the CMM (Shellard 1974). A list of organizations involved in icing problems is included in Table I.

It is difficult to extract general engineering data from the literature for predicting ice accumulation rate, extent, and frequency for a structure, since most icing reports and the few controlled experiments are specific for ship type. The factors of ship geometry – freeboard, amount of rigging and other ice-collecting surfaces above the deck, ship direction relative to the wind, and wave action – all contribute to icing severity.

Table I. Organizations involved with ship icing (provisional).

Intergovernmental Maritime Consultative Organization, London, England (b)
U.S. National Oceanic and Atmospheric Administration (c)
Meteorological Institute, Norway (c)
U.S. Navy Oceanographic Office (a)
National Research Council, Canada (a, b, c)
Meteorological Service, Argentina (c)
Meteorological Service, Federal Republic of Germany (a, c)
Meteorological Service, Iceland (c)
Meteorological Service, Japan (a, b, c)
Meteorological Office, United Kingdom (a, b, c)
Meteorological Service, Sweden (a, c)
Meteorological Service, USSR (a, b, c)

a – conducts research
b – obtains ship ice reports
c – issues warnings or forecasts ice accretion

Sea spray is a source of icing only to a height of about 50 ft above peak water level. Both fixed and floating ocean structures reach many times this height, and therefore it is necessary to consider accumulation that can occur from supercooled clouds or freezing rain. Data on accumulation from atmospheric sources are reported in the Russian literature for continental locations to a height of 300 m near Moscow. Although one of the principal factors involved in icing intensity is liquid water content (LWC) of the supercooled cloud, which varies over rather narrow limits regardless of location, it is still somewhat risky to infer maritime icing from continental data. Droplet size, extent of supply, and wind speed also have a bearing in differentiating the two environments. However, no reliable quantitative data have been reported on atmospheric icing over large bodies of water.

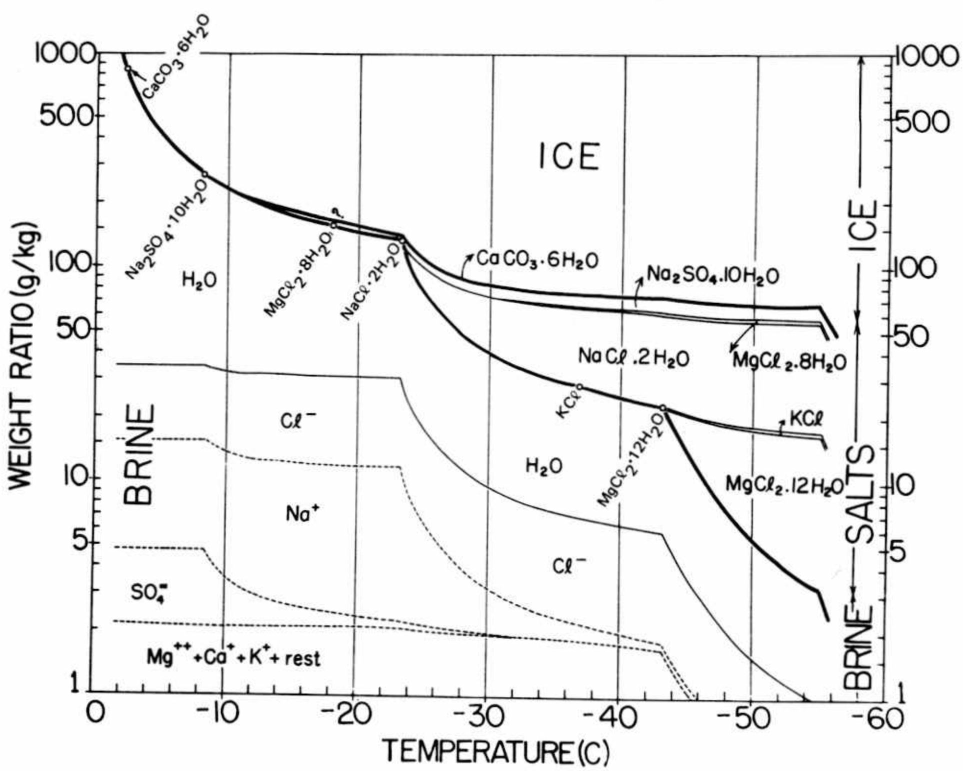

Figure 1. Phase relations for standard sea ice (Assur 1958).

Impressions from the literature include the great redundancy of the Russian sources and the perpetuation of errors which makes critical evaluation essential. For example, it is often repeated that superstructure icing will not occur at temperatures below −18°C because the water striking the ship will be in the form of small, dry ice crystals which will not adhere. Actual shipboard observations, however, have reported that icing can occur at temperatures as low as −29°C. This erroneous conclusion apparently stemmed from the British Shipbuilding Research Association experiments.

THE FREEZING PROCESS

Ice will form when a supply of water is exposed to some process which extracts thermal energy to a point where crystallization is initiated. The transition from the disordered water structure to the highly ordered ice structure requires some stimulus to trigger it; in the absence of any stimulus, fresh water can be supercooled to between −30° and −40°C before it will spontaneously freeze. The freezing process can be initiated by a mechanical stimulus such as vibration, or by the presence of nucleating centers such as dust, an ice crystal, or impurities on the walls of a vessel containing the water.

Water with dissolved impurities will freeze at a temperature below that of pure water, the depression being related to the amount of impurity. "Standard" sea water, for instance, has a salinity of 34‰ (parts per thousand) and will commence to freeze at approximately −1.9°C. The freezing front rejects the salts in the sea water and pure ice remains in the solid phase. If the concentrated brine that results cannot drain away, brine pockets form which have a lower freezing point. The incorporation of brine pockets weakens the ice structure. Sea water freezing on vertical surfaces generally forms a conically-shaped ice mass, larger at the bottom, because the droplets freezing at the top reject the brine which then drains to the lower part of the surface prior to freezing. The ice on the lower part of a structure will have a higher brine content and therefore will be weaker and may adhere less strongly to the surface. About 75% of the water in sea water will become ice before the second salt ($Na_2SO_4 \cdot 10H_2O$) crystallizes from the resulting brine at −8.2°C. The concentrations of six major ions increase until this temperature is reached. A phase diagram for sea water is presented in Figure 1.

Ice forming on structural surfaces above or close to a body of water arises principally from sea spray, with lesser sources from atmospheric precipitation (freezing rain and wet snow) or fog (arctic sea smoke, white frost, black frost). Sea spray, the most dangerous source of icing, is produced by breaking of waves against obstacles such as ship hulls, other floating objects, or shore structures, and by several different mechanisms not yet completely understood. These latter mechanisms include direct shearing of droplets from wave crests, the bursting of bubbles produced by breaking waves, and the aerodynamic suction of droplets from the crests of capillary waves (Lai and Shemdin 1974). The diameter of droplets generated by waves breaking against a ship ranges from 1.0-3.5 mm, with an average of 2.4 mm (Borisenkov and Panov 1972). In contrast, atmospheric water (cloud) droplets range in size from 5-100 μm with a median of 20 μm, and spray from wave crests has a size range of 60 μm-1 mm (see Table II).

British and Netherlands weather ships have found that a rain gauge located at a level above 16 m collected insignificant amounts of sea spray (Commission for Maritime Meteorology 1962).

Ice formed from atmospheric sources is generally free of brine inclusions. Three principal types of ice can accrete depending on wind speed and air temperature: glaze, hard rime, and soft rime. Their properties and occurrence are summarized in Table III, and data from ice accumulation in a Japanese mountain environment are graphed in Figure 2. In addition, mixtures of glaze-hard rime, glaze-wet snow, hard and soft rime, and glaze-soft rime can occur. Their properties will vary within the ranges of their components.

Table II. Characteristics of icing sources.

Source	*Droplet diameter range (μm)*	*Mean droplet diameter (μm)*	*Liquid water content (g/m³)*	*Droplet concentration per cm³*	*Reference*
Sea spray					
Breaking waves	1000-3500	2400	4600		Borisenkov and Panov (1972)
Wave crests	60-1000				Borisenkov and Panov (1972)
Fog					
Advection	6-64	20	0.17	40	Kocmond et al. (1971)
Radiation	4-36	10	0.11	200	Kocmond et al. (1971)
"Sea fog"	?-120	46	0.13		Houghton and Radford (1938)
Cloud					
Stratus	1.5-43	4.9	(0.05-0.25)		Pilié and Kocmond (1967) (Borovikov et al. 1961)
Cumulus (cumulonimbus)	4-200	40	2.5	72	Weickmann and aufm Kampe (1953)

Table III. Types of ice from atmospheric sources.

Type of ice	*Appearance*	*Density (g/cm³)*	*Conditions of formation*
Glaze	A hard, well-bonded, generally clear homogeneous ice	0.7-0.9	Supercooled water droplets at a temperature close to freezing (0° to −3°C) and wind speeds of 1-20 m/s
Hard rime	A hard, granular white or translucent ice growing in the direction of the wind	0.1-0.6	Supercooled water droplets at a temperature of −3° to −8°C, wind speeds generally 5-10 m/s
Soft rime	A white, opaque, granular ice with delicate structure only loosely bonded, growing in the direction of the wind	0.01-0.08	Supercooled water droplets at a temperature of −5° to −25°C and low wind speed (1-5 m/s)

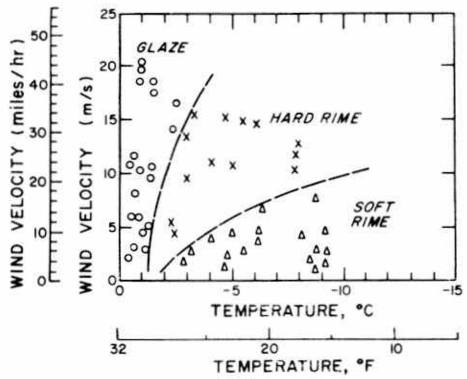

Figure 2. Relationship between meteorological conditions and type of icing (Kuroiwa 1965).

Flooding of horizontal surfaces by wave action (e.g. ship decks) usually is not a source of ice. An ice mass may result if the water cannot freely drain and becomes ponded, but very often the flushing action of huge volumes of water will wash away ice which has not yet become firmly bonded to any surface. The subject of freezing water on wooden ship decks is discussed by Kliuchnikova (1971).

ICING OBSERVATIONS

Ship icing

Statistical analysis (Borisenkov and Panov 1972) of more than 3000 cases of ship icing indicates that the principal cause of icing is spray from ocean water (89%). The combined sources of spray and fog, rain, or drizzle accounted for only 6.4% of the cases, and water spray and snow only 1.1%. The cases of icing attributable only to fog, rain or drizzle account for 2.7%. Tables IV and V (from Borisenkov and Pchelko 1972) show the distribution of icing occurrences for various regions as a function of air and water temperatures, wind speed and direction, and wave height.

Icing rarely occurs at air temperatures above 6°C, and has been recorded at temperatures below −25°C. Shekhtman (1968) has related ice accretion rate with wind speed; his analysis is summarized in Table VI. Japanese work (Tabata et al. 1963) has also related icing severity with air temperature and wind speed (Fig. 3). Three classes of icing – none, significant, and heavy – correspond to the Russian growth rate classification of Table VI. In general, the lower the air temperature and the higher the wind speed, the more likely icing will occur and the greater the severity. Ice thickness reached 20 cm in 50% of the cases. Deck accumulation from spray and snowfall reached a maximum of 100 cm.

Russian experiments and observations over three winters on ships in the Sea of Japan, Barents Sea and Baltic Sea established ranges of icing activity (Borisenkov and Pchelko 1972). Air temperatures down to −3°C were not accompanied by significant icing. At relatively low wind speeds (7-10 m/s) and air temperatures below -3°C the bow part of the ship becomes iced (for example, see cover photograph). The remaining parts of the ship accrete only slight

Table IV. Distribution of ice incidence (%) for Russian ships in various seas as related to air and water temperatures (Borisenkov and Pchelko 1972).

	Air temperature (°C)					*Water temperature (°C)*					
Sea	*0.00-4.0*	*–4.1-10.0*	*–10.1-15.0*	*–15.1-20.0*	*No. of cases*	*–2.0-1.1*	*–1.0-0.0*	*0.1+3.0*	*3.0+6.0*	*+6.0*	*No. of cases*
Bering Sea	15	60	23	2	560	6	6	78	10		517
Sea of Okhotsk	19	64	12	5	340	20	26	50	4		297
Sea of Japan and Tatarskiy Strait	13	54	27	6	201	15	14	52	4	4	192
Western Pacific Ocean	27	63	10		251	16	19	55	10		239
Barents Sea, Norwegian Sea	11	72	16	1	663	2	3	45	49	1	573
Baltic Sea	56	33	11		46		11	89			36
Labrador region	21	55	18	6	90	11	32	49	8		82
Black Sea and Sea of Azov	23	36	41		22		24	48	28		21

Table V. Distribution of icing incidence (%) for Russian ships in various seas as related to wind direction and wave height (Borisenkov and Pchelko 1972).

Sea	Wind direction and speed (m/s): 271-360° <10	>10	00-90° <10	>10	91-180° <10	>10	181-270° <10	>10	No. of cases	Wave height (m): 1-3	>3	No. of cases	Period of ships' icing
Bering Sea	12	43	16	23	1	1	2	2	567	55	45	484	Oct-Mar
Sea of Okhotsk	19	34	3	10	1	3	10	20	323	73	27	257	Oct-Mar
Sea of Japan and Tatarskiy Strait	23	55	5	9			1	7	199	82	18	151	Dec-Feb
Western Pacific Ocean	15	52	1	8	1	2	6	15	232	71	29	185	Nov-Feb
Barents Sea, Norwegian Sea	2	9	7	14	19	20	9	20	638	78	22	525	Dec-Mar
Baltic Sea		24		32	22		22		45	79	21	45	Jan-Mar
Labrador region	21	48	2	2	1	2	12	12	87	67	33	43	Dec-Feb
Black Sea and Sea of Azov	55			45					11				Jan-Mar

Table VI. Frequency (%) of icing intensity related to wind speed (Shekhtman 1968).

Icing intensity	Wind speed (knots): 0-2	3-10	11-20	21-29	30 and over	Avg. speed (knots)	No. of cases
Fast growth	2	4	12	42	40	29	15
Slow growth	1	8	29	43	19	23	303
No change	2	22	39	24	13	17	54

amounts of ice, or do not accumulate any at all. Strong winds (15–25 m/s) and air temperatures to -15°C result in ice accretion on the main deck, rigging, mast and spars, bow companionway, and bridge. Maximum deposition occurs on the main deck and trawling winch. The upper bridge and the boat deck accumulate very little ice. The ship's stern does not become iced even when the heading is downwind.

Distribution of the ice over the ship tends to be very erratic. Investigations on the *Professor Somov* in January-February 1968 established the following pattern of ice distribution: 30-70% on the horizontal surfaces, 15-40% on the vertical surfaces, 5-30% on surfaces of complex configuration (instruments and equipment), and 0-30% on the round surfaces such as mast, spars, and rigging. In the presence of spray, ice accretion commences immediately at temperatures below -3°C on the metal surfaces of the ship and on canvas equipment covers. However, ice does not form immediately on the wood decks; instead, a slush develops which mixes with sea water and flows overboard through the freeing ports. For a period of 1½ to 2 hours after formation on metal and canvas surfaces, the ice is loosely bonded and can be easily knocked or scraped off. After that time the ice becomes very tightly bonded to the surfaces and can be removed only with great difficulty.

Since a ship can present different aspects to the wind and spray source, it is to be expected that the amount of spray reaching the ship will vary. Russian observations (Kultashev et al. 1972) showed that the greatest frequency of spray, and therefore icing, occurs when a ship is heading into the wind at an angle between 15° and 45° (Fig. 4 and 5). Asymmetrical icing occurs under this condition, with the greater accumulation on the windward side. Lesser icing occurs with the ship headed directly into the wind, and then accumulation tends to be uniform. At wind speeds up to

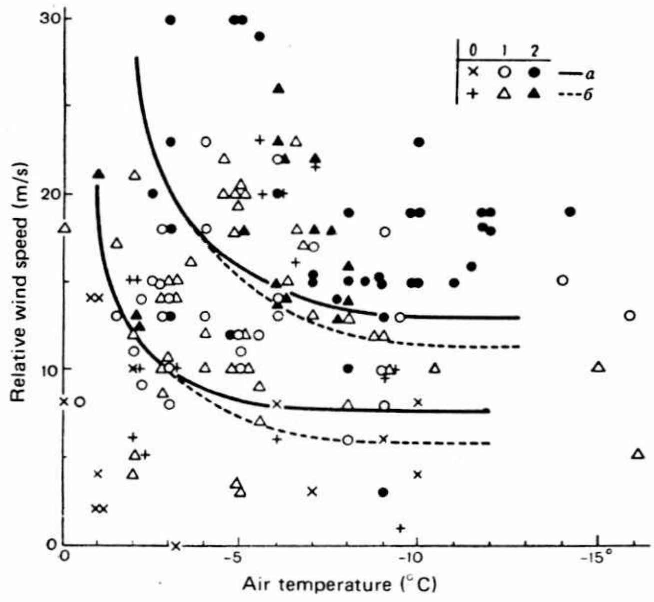

Figure 3. Icing severity as related to air temperature and wind velocity (Borisenkov and Panov 1972, taken from Japanese data in Tabata et al. 1963) where a = 450-ton displacement ship; b = 350-ton displacement ship; 0 = no icing; 1 = significant icing; 2 = heavy icing.

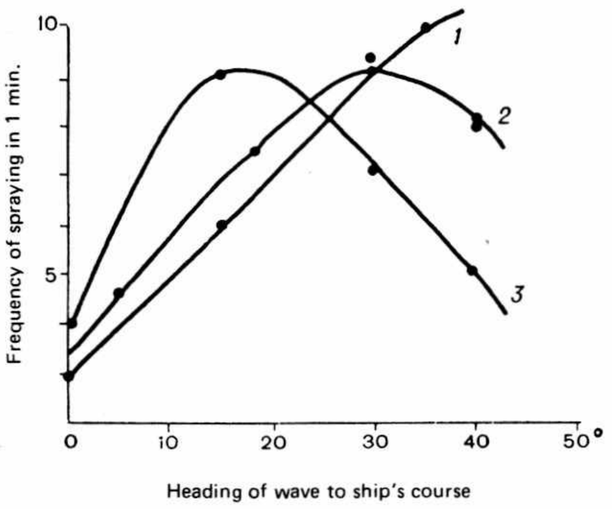

Figure 4. Dependence of spray intensity on a ship (SRT Academik Ber) on heading and wave height (1) 1.0-1.5 m; (2) 2.0-2.5 m; (3) 3.0-3.5 m (Kultashev et al.).

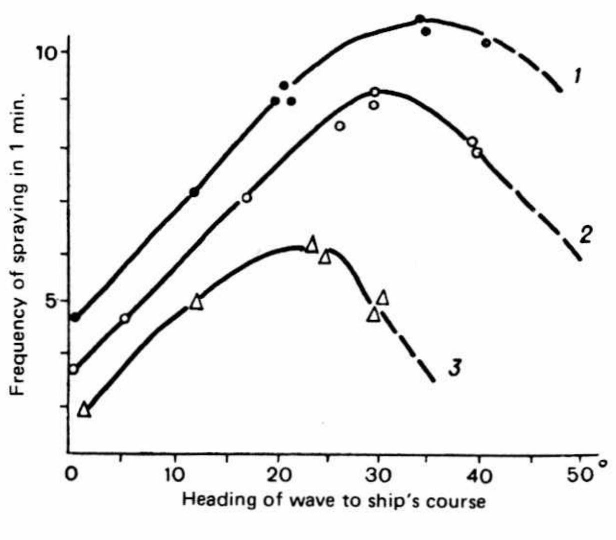

Figure 5. Dependence of spray intensity on speed of ship and wave heading (Kultashev et al.). Speed of ship in knots: (1) 8.5; (2) 7.0; (3) 5.5.

20-25 m/s ice accumulation occurs mainly on the forward half of the vessel, including the front and side walls of the superstructure and bridge wings. These observations were made on medium-sized fishing trawlers.

Details of the observations are not given in (Kultashev et al. 1972), and it is not immediately evident why low wave heights will result in the greatest spray intensity (Fig. 4). It is likely, however, that the hull of a ship as small and with as low freeboard as the SRT will bob with the higher waves and not crash into them. The relationship between spray intensity and ship speed is clearer: a greater beam heading of waves is necessary at higher speeds for waves to break, and then their greater impact results in greater production of spray (Fig. 5).

The British Shipbuilding Research Association model tests also showed the influence of wind heading on icing severity. The quantitative results and icing rate are subject to question, but the relative degree of icing is credible. The model was floated in water whose temperature was kept at 1.1°C and the air temperature was kept at -10°C to -6°C. The wind speed simulated 45-55 knots. Spray was created by injecting (fresh) water into the room by compressed air and spray nozzles. Tests were carried out with the model in three positions, first with normal rigging then with a tripod mast. The results were as follows:

1. Head to wind. The model iced steadily until it capsized. The greatest weight of ice it could carry and remain upright in calm water was equivalent to about 145 tons on the 180-ft-long × 30.5 ft-beam full-scale ship (1,115 ton displacement). The rate of loss of metacentric height with normal rigging was roughly linear for the first 100 tons of accumulated ice on the full-scale ship. This fell off and reached a maximum loss of 17 in. when 150 tons was deposited. The metacentric height was 20 in. without ice. With a tripod mast the loss in metacentric height was only $^2/_3$ the loss with normal rigging for a given ice weight and the center of gravity was about 5 ft lower.

2. Stern to wind. There was heavy ice buildup aft, and very little forward, of the bridge. The loss of metacentric height was half that which occurred head to wind because of the sheltering of the foremast by the superstructure.

3. Thirty degrees to the wind. Ice accumulated on the windward side and caused heeling into the wind. This resulted in increased accumulation in the upper rigging, and the model capsized, carrying less than half the ice burden of the head to wind position.

Shellard (1974) summarizes conditions for icing due to sea water. These occur whenever sea spray is present at the same time that the air temperature, and therefore the temperature of most exposed surfaces, is below the freezing point of sea water. The freezing point will vary from a little below 0°C for only slightly saline waters to −1.9°C for ocean water. A small vessel is likely to begin generating spray in a sea corresponding to force 5 (17-21 knots), and at force 6 (22-27 knots, with wave heights of 3 m or more) most small vessels moving against the waves will be showered in spray. Spray blown from wave tops is not likely to become a serious source of icing, however, until much higher wind speeds are reached, because such spray is patchy and at a low level when it begins to appear at 17-27 knots. As a consequence, it will not likely be blown in large amounts to deck level until at least force 9 (41-47 knots) is reached, i.e. at the point where visibility begins to be affected. These observations can be applied to fixed installations which may not generate quantities of the larger droplets from impacting waves.

Woodcock (1953) reports that foam patches resulting from white caps at the sea surface remained visible from an aircraft for more than two minutes in a force 5 wind in the Hawaiian area, which supports Shellard's comment regarding the initiation of spray icing at that wind speed.

Russian sources (Borisenkov and Pchelko 1972, Borisenkov and Panov 1972) describe three classes of icing for medium-size fishing trawlers (type SRT, 30-40 m long, 300-500 tonnes displacement, 23-26 man crew). These are:

1. Gradual icing – accretion rate is not more than 1.5 tonnes/h. It occurs during sea spray or atmospheric precipitation (rain, fog, frost smoke), at any wind speed when air temperatures range from −1° to −3°C, and at wind speeds of 0-9 m/s with air temperatures below −3°C.

2. Rapid icing – icing rate is 1.5–4 tonnes/h. It occurs at wind speeds of 9–15 m/s and air temperatures of -3 to -8°C.

3. Very rapid icing – icing rate is more than 4 tonnes/h. It occurs at wind speeds above 15 m/s when the air temperature is below -3°C or at wind speeds of 9-15 m/s when the air temperature is below −8°C.

Mertins (1968) analyzed 400 observations of ship icing due to sea spray in the seas around Iceland, Greenland, Labrador, and northwestern Russia, and related the severity of ice accumulation to wind speed, air temperature and sea water temperature (the oceans involved all have salinity of 30-34$^0/_{00}$, with initiation of freezing at -1.9°C). He translated these relationships into the graphs given in Figure 6.

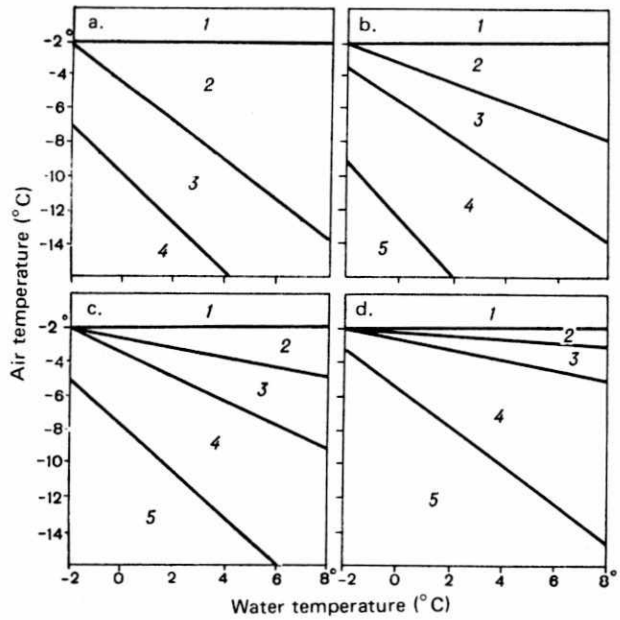

Figure 6. Graphs for determination of ice accretion on fishing vessels at low speeds (Mertins 1968). Numbers indicate icing severity: 1 – none, 2 – light (1-3 cm/24 h), 3 – moderate (4-6 cm/24 h), 4 – severe (7-14 cm/24 h), 5 – very severe (≥ 15 cm/24 h). Wind force:

	Beaufort	*Knots*
a.	*6-7*	*22-33*
b.	*8*	*34-40*
c.	*9-10*	*41-55*
d.	*11-12*	*56+.*

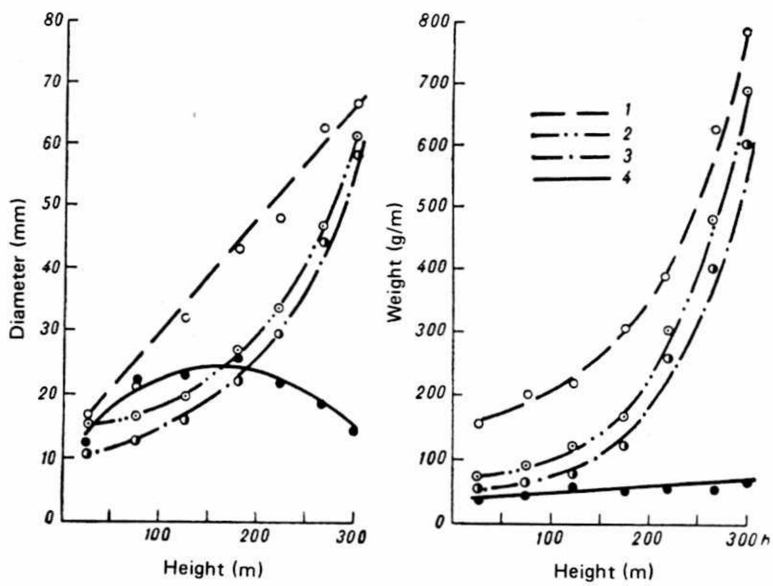

a. Average diameter vs height. *b. Average weight vs height.*

Figure 7. Variation of average diameter and weight of ice accumulation (1 – mixture, 2 – hard rime, 3 – glaze ice, 4 – soft rime) with height on meteorological tower at Obninsk, U.S.S.R. (Glukhov 1972).

Table VII. Occurrence (%) of type of ice by height on meteorological tower in Obninsk, U.S.S.R. (Glukhov 1972).

Height range (m)	Type of ice Soft rime	Glaze	Hard rime	Mixture
0-100	23	5	5	2
100-200	29	31	25	23
200-300	48	64	70	75
No. of cases	227	237	633	396

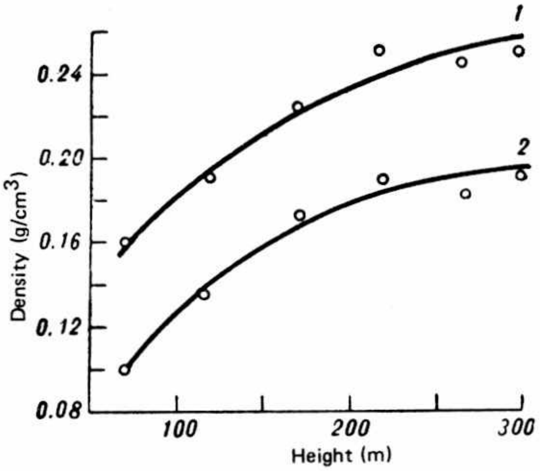

Figure 8. Variation of density of ice accumulation (1 — mixture, 2 — hard rime) with height on meteorological tower at Obnisk, U.S.S.R. (Glukhov 1972).

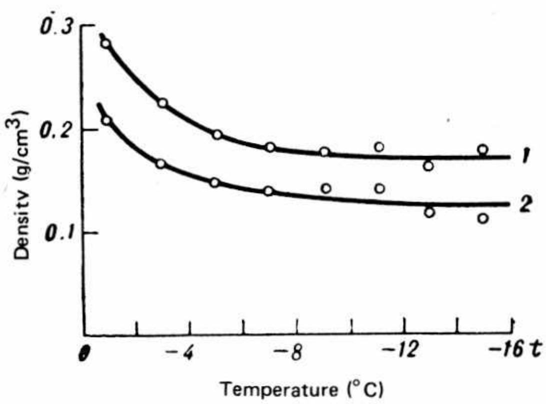

Figure 9. Dependence of density of ice deposit (1 — mixture, 2 — hard rime) on air temperature on meteorological tower at Obninsk, U.S.S.R. (Glukhov 1972).

Atmospheric icing

Detailed observations of icing occurring up to a height of 300 m on a meteorological tower at Obninsk, near Moscow, have been made and are reported in the literature (Glukhov 1972). The type of icing that occurred in three height zones is given in Table VII. Up to a height of 100 m soft rime predominated. The thickness of the accumulation, and the weight observed are plotted in Figure 7 as a function of height for the four types of icing. The densities of the two types of ice which accumulate most heavily, the mixed ice and the hard rime, are plotted as a function of height in Figure 8 and as a function of air temperature in Figure 9.

GEOGRAPHICAL DISTRIBUTION OF ICING AND CONTRIBUTING METEOROLOGICAL CONDITIONS

As a rule, icing of ships in the northern temperate latitudes takes place during the intrusion of cold air masses in the autumn, winter, and spring (Table VIII). This usually occurs in the rear of low-pressure areas with north, northwest and west winds; it occurs less frequently in the forward part of a low during northeast or east winds (Table IX). The advection of cold air into the back edge of a low accompanied by relatively strong winds is one of the typical conditions during icing incidents. The icing zone at the rear of a low does not start immediately after passage of the cold front because the air temperature directly behind the front has not yet reached the low values necessary for icing. In addition, following the passage of a cold front, a change of wind direction and speed generally occurs which leads to a weakening of the wave action (lower swell).

Extreme icing conditions

The most extreme cases of superstructure icing reported in the Russian literature have taken place during February in the Barents Sea between Norway and

Table VIII. Period and frequency of Soviet ship icing (Borisenkov and Pchelko 1972).

Region	No. of cases	Period of icing	Frequency (%)
NW part of Atlantic	85	15 Dec–15 Mar	92
Norwegian and Greenland Seas	109	15 Dec–31 Mar	77
Northern part of Atlantic	63	15 Dec–15 Apr	92
Barents Sea	390	1 Jan–15 Mar	78
Baltic Sea	21	15 Dec–29 Feb	85
Baffin Sea, Hudson Bay	7	1 Dec–31 Mar	96
Newfoundland region	15	1 Jan–15 Mar	79
Bering Sea	185	1 Dec–31 Mar	70
Sea of Okhotsk	337	1 Dec–31 Mar	70
Sea of Japan	226	1 Dec–29 Feb	85
NW part of Pacific	183	15 Dec–31 Mar	79
Arctic seas (Kara, Laptev, East Siberian and Chukchi)	71	15 Jun–15 Nov	100

Table IX. Synoptic conditions at time of ship icing (Russian observations 1967-69), from Borisenkov and Pchelko (1972).

Sea	Rear of low-pressure area (%)	Forward part of low (%)	Other conditions (%)	No. of cases
Bering Sea	57	32	11	442
Sea of Okhotsk	70	23	7	312
Sea of Japan, Tatarskiy Strait	93	3	4	140
Western Pacific Ocean	75	19	6	182
Barents and Norwegian Seas	40	50	10	596
Baltic Sea	4	66	30	44
Black Sea and Sea of Azov	79	16	5	18

Spitzbergen (the region of 74°35′N, 19°40′E). Twenty-eight of 48 reported icings with thickness greater than 10 cm and 8 of 10 cases with thickness greater than 20 cm occurred in February (Kaplina et al. 1972). The February weather in this region is characterized by great temperature contrasts in the surface sea temperature and in the lower layers of the atmosphere. A vast cyclonic region occupies the space between the southern tip of Greenland and the Kara Sea, and the influence of this zone extends to the North Pole and the Laptev Sea. The periphery of depressions is generally characterized by large horizontal pressure gradients and high winds. Detailed examination of four cases of intense ship icing (ice thickness 20-40 cm) revealed a general pattern: all the ships were on the northern edge of a vast multicentric depression; in three cases the ships were in a warm front, and only one in a cold front. Significant horizontal temperature gradients, sometimes reaching 7–8°C/degree latitude, were measured. During icing the ships were on the western side of the cold air wedge, in a region of increasing horizontal air temperature differences.

Extremes of ice accumulation

A glaze storm on 27-29 January 1940 struck Great Britain and resulted in some of the greatest accumulations of ice ever recorded: 6 in. of ice on an automobile and 4 in. on twigs in Worcestershire, and 2.4-in.-diam accumulation on a telegraph wire in Wiltshire. The maximum thickness reported in a series of observations in Russia in the 1920's was a diameter of 114 mm on a 5-mm wire in Tokmak in the Kirghiz (Bennett 1959). Ice that accumulated to a diameter of 25 cm on guy wires of a tower in Newfoundland was estimated to have weighed over 40 kg/m (Boyd and Williams 1968).

Prediction of icing occurrences

A summary of Russian experience would incorporate the following factors for the prediction of icing occurrences:

1. The greatest threat exists in the rear of a low pressure system, and to a lesser extent in the forward part. (In both cases, it is recommended that the active advection of cold air at heights of 1.5-3 km be recorded during periods of strong winds and negative air temperatures.) Icing occurs relatively less often in lows during east, southeast, and south winds.

2. Sea spray icing conditions require a strong wind, blowing for a relatively extended period (3-6 h or more) in one direction. Floating ice will prevent the development of waves and eliminate spray as a source of icing. During an offshore wind, icing of ships will not occur within a distance of 1-3 miles from shore, depending upon the height of the shore.

3. The icing zone at the rear of a low usually does not begin immediately, but at some distance behind the cold front.

4. A zone of very rapid icing of ships develops in the vicinity of a cold trough at the 850-mbar level, particularly when the temperature at that level reaches −18°C and is dropping.

5. In the northern part of the Atlantic Ocean and in the Barents Sea, which are influenced by the Gulf Stream, it is necessary to take into account the temperature of the surface water layer if it is higher than 2°C.

The Russian literature presents a confusing picture regarding the probabilities associated with occurrence of icing. Locations of reported icing incidents are less questionable, as is shown in Appendix A for the North Pacific Ocean and Far East waters. Other indicators of probabilities are less precise and sometimes contradictory. This probably results from observations made on different types of vessels with differing sail areas and therefore varying total ice accumulations and rates. The Russians have attempted to develop empirical factors to relate calculated parameters to observed icing accumulation.

The maps in Appendix A, which have appeared in the literature, show icing probabilities for various regions and climatological conditions. Other sources of icing charts are published by the U.S. Navy (1958, 1963) and the National Aeronautics and Space Administration (1968).

The occurrence of supercooled fogs is an indication of probable rime ice formation on exposed elevated structures. Charts have been prepared (Guttman 1971) that are based on the frequencies of fog in any form and the frequencies of freezing surface air temperatures (Fig. A9).

PREDICTION OF ICING INTENSITY AND RATE

A Russian analysis for predicting icing intensity on ships is based on a heat balance equation of the surface subjected to the icing (Borisenkov and Pchelko 1972). The intensity I (g/cm^2 h) of ice accretion on a 1-cm^2 surface normal to the spray flow is computed from

$$I = \alpha \frac{T_\ell - T_z + 2.6(L_i/p)(E_{T_a} - E_{T_\ell})}{L_z + C_\ell(T_a - T_\ell) + C_w(T_\ell - T_z)}$$

where α = heat transfer coefficient dependent on wind speed and configuration of icing surface (Fig. B1)

L_z, L_i = heat of fusion and vaporization of ice, respectively (Table BI)

C_ℓ, C_w = specific heat capacities of ice and water, respectively (Table BIII)

T_a = air temperature

T_z = temperature of water droplets in a freshwater or sea spray cloud (Tables BIV and BV)

T_ℓ = temperature of the ice during the ice formation process

E_{T_a}, E_{T_ℓ} = water vapor pressure above water surface at temperature T_a (Table BVI), and above ice at temperature T_ℓ (Table BVII)

p = atmospheric pressure.

The equation is used for calculating both sea spray and fresh water ice accretion. In the case of sea spray, it is necessary to compute the T_z value as a function of the droplet size, time of flight, and temperature of the ambient air (Table BII). It is assumed in the case of freshwater (atmospheric) icing that the droplets will acquire the temperature of the ambient air.

Graphs of ice accumulation rate (g/cm^2 hr) resulting from various combinations of parameters are presented in Appendix Figures B2-B8 (Borisenkov et al. 1971). The use of these graphs for predicting ice burdens is explained more fully in Appendix C.

Another approach to ship icing prediction and calculation is based on the icing of an infinitely long cylinder in the flow of supercooled water droplets, in which icing intensity is related to the propagation of a freezing front. In this model the ice is assumed to build up under a film of water ("wet growth"). The solution has a simple form:

$$H = \frac{A}{B - C}$$

where A = a function of average wind speed and $T_\ell - T_a$

B = the latent heat of vaporization of ice

C = a function of the difference between the freezing point of water and the air temperature and water temperature.

H characterizes the intensity of icing of a cylinder of a certain size. To convert to the case of general icing of a ship sailing on a heading of 0-40° under the same hydrometeorological conditions, a graph is constructed. According to Russian opinion, this empirical approach is apparently the most suitable method for tying together the theoretical calculations and field observations.

A third approach considers the water droplet flux and the fraction of droplets which will strike a surface and freeze. Droplets approaching a cylinder may strike the surface or may be deflected. If the diameter of the droplets is small, they will be carried with the air stream around the cylinder and will not form an ice deposit. As droplet diameters increase so does their momentum. Their paths will deviate from the air stream, and they will impinge on the cylinder to form an ice deposit. The amount of ice deposited per unit time and length of cylinder is given by Kuroiwa (1965) as

$$\frac{dM}{dt} = 2ERVw$$

where M = the mass of supercooled water droplets which cause icing in time t

R = the radius of the cylinder

V = the wind velocity

w = the liquid water content in the air stream

E = the collection efficiency, with a value between 0 and 1.

The collection efficiency (or collision coefficient) E is defined as the ratio of the mass of water droplets striking the surface in unit time to the mass of droplets which would have struck the surface if they had not been deflected (see Fig. 10). According to Langmuir and Blodgett (1946), E is a function of two factors K and ϕ:

$$K = 1.29 \times 10^3 \frac{Vr^2}{R}$$

and

$$\phi = 0.175\ VR$$

where r = droplet radius (cm)

V = wind speed (cm/s)

R = cylinder radius (cm).

A graphical solution for E once K and ϕ are calculated is given in Figure 11. If $K \leqslant 1/8$, $E = 0$ for any ϕ. Manipulation of these equations can give the critical radius of a cylinder above which icing theoretically will not take place. A graphical solution is given in Figure 12. The actual size of cylinder will vary depending upon turbulence. The relationship has been developed for small (atmospheric) water droplets.

Russian observations of icing of a 15-mm-diam circular cylinder have resulted in the data graphed in Figure 13, where the collection efficiency E is given as a function of droplet diameter and wind speed.

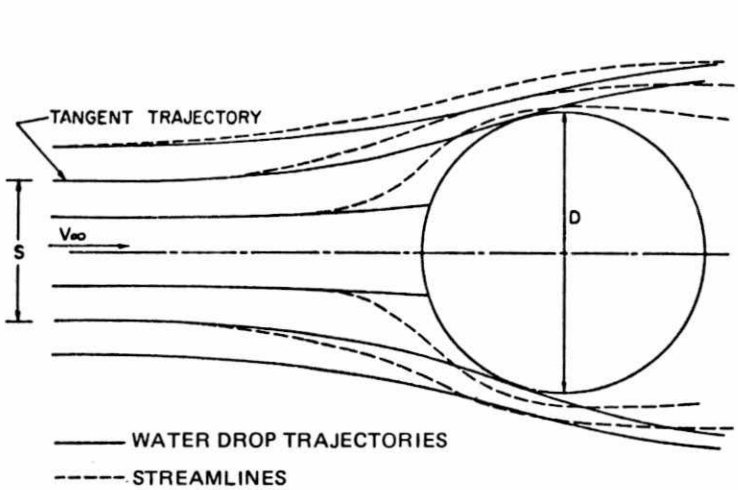

Figure 10. Collection efficiency of a cylinder. Water droplets following trajectories off the center line approach will be deflected and, at a certain distance from the axis, will not impinge on the cylinder. Collection efficiency is the ratio of the mass of droplets striking the cylinder to the total mass that would impinge if they were not deflected. If a constant mass flux is assumed, this can be represented in terms of the linear measures S and D, so that E = S/D (Stallabrass and Hearty 1967).

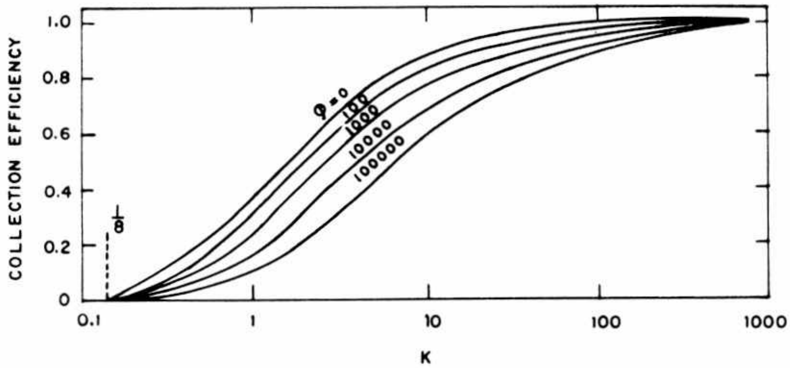

Figure 11. Collection efficiency E is determined by an inertia parameter K and the parameter ϕ (Langmuir and Blodgett 1946).

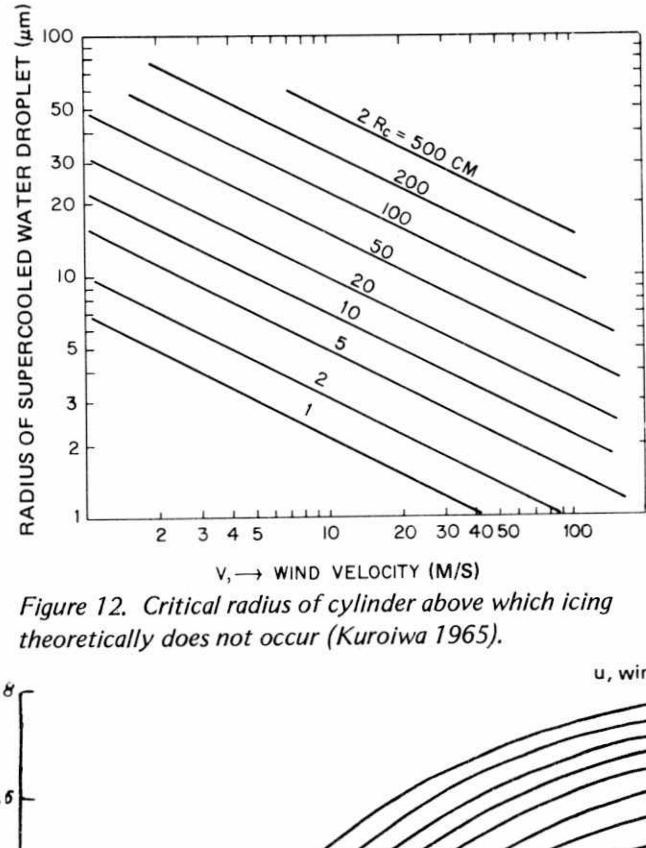

Figure 12. Critical radius of cylinder above which icing theoretically does not occur (Kuroiwa 1965).

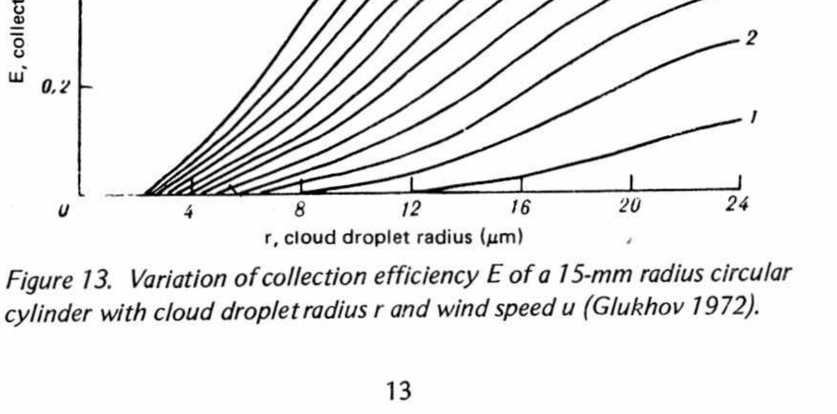

Figure 13. Variation of collection efficiency E of a 15-mm radius circular cylinder with cloud droplet radius r and wind speed u (Glukhov 1972).

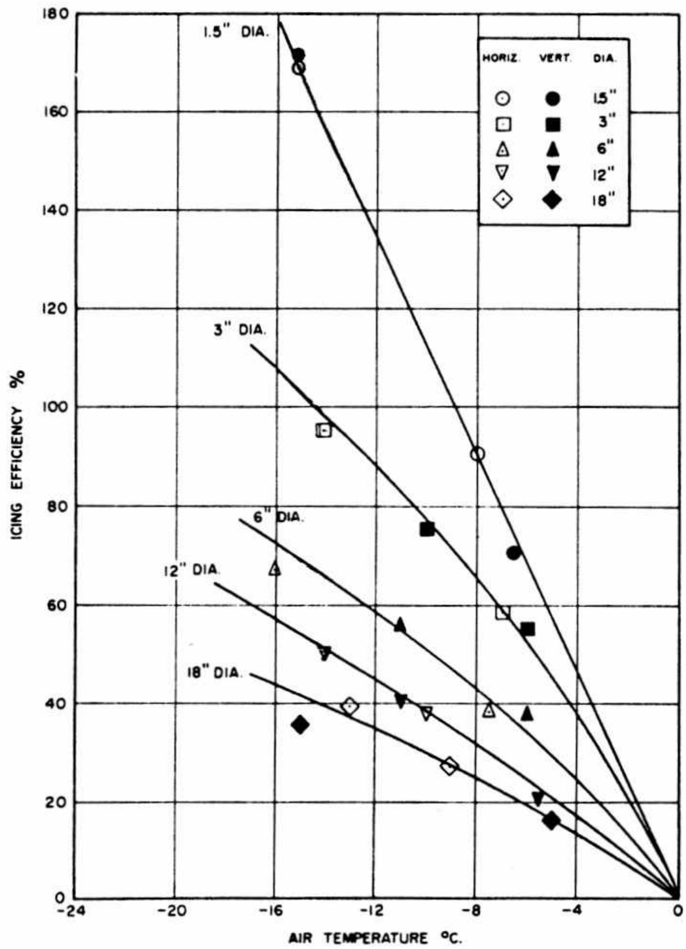

Figure 14. Icing efficiency, i.e. the fraction of water droplets that could strike a cylinder if not deflected and which will freeze on the surface, as related to air temperature and diameter of cylinder. Small cylinders, below 3 in. in these experimental results, will form ice exceeding the original diameter of the cylinder when temperatures are low enough (Stallabrass and Hearty 1967).

This shows the sizes of droplets that will impact on a cylinder at a given wind speed.

Not all the droplets striking the obstacle, whether supercooled or not, will freeze and be retained on the obstacle. Stallabrass and Hearty (1967) define an "icing efficiency" as the product of the collection efficiency and the freezing fraction. They conducted ice accumulation tests in an icing wind tunnel and measured a one-hour average icing efficiency. Their results, some of which are shown in Figure 14, graphically depict the great influences of cylinder diameter and temperature upon ice accretion. (Test conditions were: air speed 50 mile/h, air temperature between -16° and -5°C, water concentration 3.2 g/m^3, and median droplet diameter 200 μm.)

Wind speed influences not only the collection efficiency but also the freezing fraction. With increasing wind speed the icing efficiency (or capture coefficient as it is called in the Russian literature) increases to a maximum and then drops off gradually. The trend, plotted from Russian observations and shown in Figure 15, results not from a reduction in the collection efficiency but from change in the freezing fraction. (In fact, as is evident from Figure 11, collection efficiency E approaches 1 as K increases, and K is a linearly increasing function of wind speed.) At low wind speeds nearly all the droplets which collide with the surface will freeze because the heat of fusion can be dissipated to the surroundings. As more and more droplets strike the surface with increasing wind speed, however, the

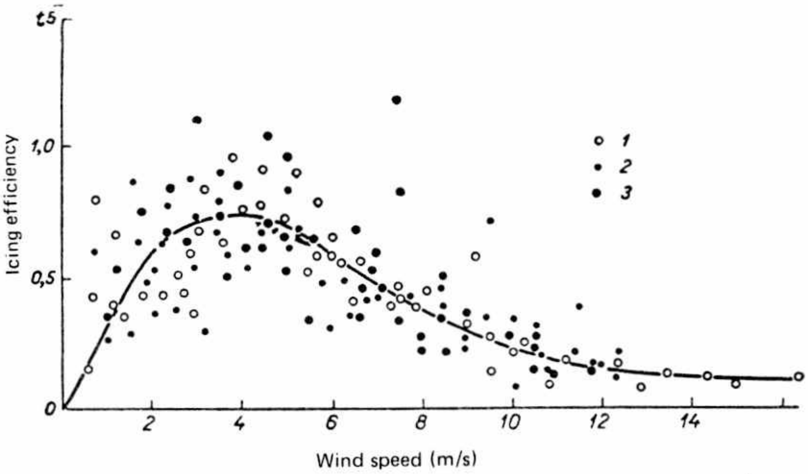

Figure 15. Dependence of icing efficiency (or capture coefficient) on wind speed for various liquid water contents w (Glukhov 1971), where 1) w = 0.12–0.16 g/m^3, 2) w = 0.17–0.21 g/m^3, 3) w = 0.22–0.26 g/m^3.

heat of fusion cannot be dissipated rapidly enough. Some droplets will remain in the liquid state and flow to the outer surface, there to be entrained by the air flow and carried away.

CONTROL METHODS

No completely effective methods of ice accretion control or removal have been found. Mechanical (impaction) methods are the most common techniques, but experiments have been conducted on heated surfaces, icephobic surfaces, deformable surfaces, and freezing point depressants. Also, no device for unequivocal remote measurement of ice accumulation rate is available, though some techniques are available for such measurements under experimental conditions. In critical areas, where no ice accumulation can be accepted, or where accumulation beyond a certain point may lead to catastrophic failure, active control methods must be used. Application of heat is the most dependable but not necessarily the most convenient, practicable, or cost-effective method, because irregular surfaces, surfaces exposed to very high heat losses, and extensive areas all present problems. Therefore, heating can be considered for use only in certain areas.

Methods of removal of ice accumulations reported in the literature are conventional: baseball bats, sledge hammers, axes, hammers, picks, and other impact instruments are frequently mentioned as the only tools available, but icephobic coatings and heated surfaces have been experimented with. By itself, an icephobic or low-energy surface may be insufficient to reduce ice accumulation.

Stallabrass (1970) investigated a number of methods of reducing accretion of ice on ships. The methods utilized, in order of their deicing effectiveness or ease of ice removal, were:

1. Pneumatic deicer
2. Freezing point depressant (ethylene glycol)
3. Rubber-surfaced plastic foam on steel panel
4. Gray deck paint on wooden panel
5. Spar varnish on wooden panel
6. Bare polyethylene foam on steel panel
7. Black rust-preventive paint on steel panel
8. Gray deck paint on steel panel.

The tests were made in an icing wind tunnel and on outdoor (land) test sites, and were very qualitative. In addition, a polyethylene-sheathed parallel filament rope was compared with a steel cable for ice accretion and removal. Because of the lower torsional stiffness of the rope, it tended to twist during the icing event and to accrete around the entire circumference, in contrast to the steel cable which presented a constant face to the airborne droplets and therefore built up asymmetrically. Little difference was noted in the ease of removal of ice from the polyethylene-sheathed rope compared to the steel cable, because of the encapsulation of the plastic.

The 4- × 3-ft pneumatic deicer worked effectively when attached to both a 1-ft-diam cylindrical form simulating a mast and when spread flat on a panel.

According to Bates (1973), Santomelt 990-CR (an organic freezing point depressant manufactured by Monsanto Co.) was used very effectively on the *USCGC Burton Island* to keep the flight deck, turnbuckles, shackles, and lines clear of ice.

An item in a popular Russian publication (Soviet Life 1975) reports that their scientists have suggested the use of an anti-icing "shirt" for protection against ship icing, and that tests have proved the effectiveness of the method. It is quite likely that this is merely a flexible plastic sheeting covering portions of the superstructure.

Ice and snow accumulation on power line towers in Norway has been reduced by enclosing monolithic concrete structures as well as open-lattice steel towers with sheets of solid, corrugated plastic. This technique may be applicable to ocean installations.

Since sea spray is the principal source of icing, reduction of the supply of spray from breaking waves is an obvious control strategy. Wave damping would be required for the maximum distance that a droplet would travel. Large (1 to 3.5-mm) droplets generated by wave impaction, rather than spray whipped off breaking swell waves, are of primary concern. Droplet size of the latter averages 200 μm (Wu 1973). Borisenkov and Panov (1972) state that the flight time of droplets generated by a ship plowing into waves is 1.3-1.4 s until impact on the ship. Since this presumably is the forward part of the ship, total flight time until the drop reaches the sea again is reasonably estimated as 6 s. In a 30-m/s wind, a drop would travel 180 m. A small droplet, 200 μm and below, would travel a much longer distance. It is not likely that it would be economical to install wave damping for such a large area.

Deflection of droplets from a trajectory that will carry them to a surface to be protected may be possible. This may be accomplished by an air curtain, or by another surface whose shape can be given optimum aerodynamic design or which may be permitted to accumulate ice. This approach is experimental and requires design for specific conditions.

Heated water is used for flushing decks and other surfaces for ice removal. However, large quantities of sea water even slightly above the freezing point can be used for removal or protection if cooling due to wind is not excessive and if proper drainage is provided to prevent ponding.

DeAngelis (1974) presents a list of suggestions for reducing ice hazards to ships that originated in a Russian proposal to IMCO. The suggestions are:

1. The ship should be headed toward warm water or protected coastal areas.

2. All fishing gear, barrels, and deck gear should be placed below deck or fastened to the deck as low as possible.

3. Cargo booms should be lowered and fastened.

4. Deck machinery and boats should be covered.

5. Storm rails should be fastened.

6. Grating should be removed from scuppers, and all objects that might prevent water drainage from the deck should be moved.

7. The ship should be made as watertight as possible.

8. If freeboard is high enough, all empty bottom tanks containing ballast piping can be filled with seawater.

9. Reliable two-way radio communication should be established either with a shore station or another ship.

MEASUREMENT OF ICING RATE

Laboratory measurement of icing rates has generally been accomplished by inserting a cylinder into the droplet stream and periodically weighing it. This method has been adapted by Japanese investigators during ship observations in three variations: continuous weighing of a suspended rod by an electrical sensor, periodic removal and weighing of the rod or a similar cylinder, and the collection of brine in cups placed below vertical rods for analysis of chlorinity and inclusion of brine. Sea spray flux has been measured by the Japanese by locating rolls of toilet tissue at various points on the ship, then periodically replacing and weighing them.

The Rosemount ice detector, an automatic continuous-recording device (Rosemount Engineering Company, Minneapolis, Minnesota) was developed initially for measurements on aircraft, but has been adapted for detection and measurement of land structure icing. Detection is based on the change in resonant frequency of a small vibrating rod in the droplet stream. Sensitivity can be selected to initiate a deicing cycle when ice growth has reached a predetermined mass; the number of deicing cycles is a measure of accumulation rate. It has been tested in the rigorous climate on Mt. Washington, New Hampshire, and performed satisfactorily under principally rime ice conditions (Ackley et al. 1973). It has not been tested in a maritime environment, as far as is known.

A concept for an icing rate meter for the measurement of sea spray is proposed, based upon a design suggested by R.T. Atkins* of CRREL. This would consist of either a sphere or cylinder mounted on a thin support to which a strain gauge is attached. The sphere or cylinder would be covered with an inflatable skin. In an exposed environment, ice would form on the skin

* Personal communication, R.T. Atkins, Chief, Technical Services Division, CRREL, 1975.

and the added load would be interpreted in terms of ice thickness. Average wind speed for short periods could be obtained from integration of the signal from an accelerometer, or from measurement of the offset of the signal from the strain gauge mounted on the support arm. Periodic deicing of the meter would be accomplished by inflating the skin to break off the accumulation.

CONCLUSIONS AND RECOMMENDATIONS

1. The most common cause of icing at sea is sea spray generated primarily by wave impaction on the structure, and to a lesser extent by droplets sheared from breaking waves. Other causes of icing include freezing rain, snowfall, and fog.

2. Icing of slow-moving ships in the ocean does not generally begin until the air temperature drops to -3°C. In general, icing severity increases as air temperature decreases and wind increases.

3. Icing severity is not strongly related to sea water temperature, and icing has been reported at water temperatures around 6°C.

4. Icing increases as the wind approaches more on the beam, between 15° and 45°, then decreases.

5. Spray does not become a significant factor in icing until the wind speed reaches about 17 knots. Spray is generated by wave-top disturbance commencing at about this wind speed, but it is not carried to a very high level. Higher wind speeds are necessary (around 40 knots) before spray is carried high enough to reach deck height.

6. Small diameter cylindrical surfaces will accumulate ice more rapidly than large cylinders or flat surfaces. Design of a structure for icing environments should minimize the number of small cylindrical surfaces.

7. Distribution of ice accretion on a ship is erratic, though a beam angle will result in asymmetrical accumulation. Russian observations on a small (40-m-long) trawler showed the following distribution: horizontal surfaces, 30-70%; vertical surfaces, 15-40%; complex surfaces, 5-30%; cylindrical surfaces, 0-30%.

8. Accreted sea ice is initially only loosely bonded to a surface, but the strength of adhesion rapidly increases and approaches a maximum in 1½ to 2 hours. Thus, ice should be removed as soon as possible after accumulation.

9. Icing occurs most frequently in the rear of a low-pressure area. The icing zone following passage of a depression does not start immediately because the air temperature requires time to drop to the low level necessary for icing and because a change in wind speed and direction generally occurs and weakens wave action.

10. The presence of a cold trough at the 850-mb level, with temperatures at -18°C and falling, is strong indication of potential icing conditions at sea level.

11. No completely effective methods of control of ice accretion have been developed, and brute force (baseball bats, sledge hammers) is frequently the only available technique. Experiments have been conducted with heated, icephobic, and deformable surfaces and with freezing point depressants, but additional field experiments and developmental work are necessary.

12. No effective ice rate meter suitable for use under all conditions is available; development is recommended.

13. Insufficient information is available in the literature to provide a good estimate of water droplet flux as a function of height and wind speed. An observational program on fixed ocean installations is recommended.

SELECTED BIBLIOGRAPHY

Ackley, S., K. Itagaki and M. Frank (1973) An evaluation of passive deicing, mechanical deicing and ice detection. CRREL Internal Report 351 (unpublished).

Alexeiev, Ju. K. (1974) Protecting sensors and masts of automatic meteorological stations against icing. Technical Note 135, World Meteorological Organization.

Assur, A. (1958) Composition of sea ice and its tensile strength. In *Arctic sea ice*, U.S. National Academy of Sciences Publ. 598, p. 106-138.

Bardarson, H.R. (1969) Icing of ships. *Jokull*, vol. 19, p. 107-20.

Bates, C.C. (1973) Navigation of ice-covered waters: Some new initiatives by the United States of America. In *23rd Report, International Congress of Navigation, Permanent International Association of Navigation Congresses*, Brussels.

Bennett, I. (1959) Glaze, its meteorology and climatology, geographical distribution, and economic effects. Technical Report EP-105, Quartermaster Research and Engineering Center.

Berenbeim, D.IA. and T.G. Burukovskaia (1971) Studying icing of ships in laboratories. In *Theoretical and experimental studies of ship icing* (in Russian). Leningrad: Gidrometeoizdat, p. 108-119.

Borisenkov, E.P. (1972) Theory of ship icing from spray (in Russian). Leningrad: Arkticheskii i antarkticheskii nauchno-issledovatel'skii institut, Trudy, vol. 298, p. 34-43.

Borisenkov, E.P. and V.V. Panov (1972) Basic results and perspectives on the investigation of hydrometeorological conditions related to ship icing (in Russian). Leningrad: Arkticheskii i antarkticheskii nauchno-issledovatel'skii institut, Trudy, vol. 298, p. 5-33. Also in CRREL Draft Translation 411, AD A003215.

Borisenkov, E.P. and I.G. Pchelko, Eds. (1972) Indicators for forecasting ship icing (in Russian). Leningrad: Arkticheskii i antarkticheskii nauchno-issledovatel'skii institut. Also CRREL Draft Translation 481, AD A030113.

Borisenkov, E.P., V.V. Panov and V.N. Molchanov (1971) Results of theoretical calculations of ship icing intensity. In *Theoretical and experimental studies of ship icing* (in Russian). Leningrad: Gidrometeoizdat, p. 6-15.

Borisenkov, E.P., A.P. Nagurnyi, V.N. Molchanov and V.V. Panov (1971) Numerical forecasts of ship icing conditions. In *Theoretical and experimental studies of ship icing* (in Russian). Leningrad: Gidrometeoizdat, p. 159-165.

Borovikov, A.M. et al. (1961) *Cloud physics* (in Russian). Leningrad: Gidrometeoizdat.

Boyd, D.W. and G.P. Williams (1968) Atmospheric icing of structures. Technical Paper 275, Division of Building Research, National Research Council, Ottawa, Canada.

Buianov, N.F. (1971) Experience in operating medium-tonnage fishing boats under icing conditions. In *Theoretical and experimental studies of ship icing* (in Russian). Leningrad: Gidrometeoizdat, p. 98-107.

Commission for Maritime Meteorology (1962) Precipitation measurements at sea. Technical Note 47, World Meteorological Organization, Geneva.

DeAngelis, R.M. (1974) Superstructure icing. *Mariners Weather Log*, vol. 18, no. 1, p. 1-7.

Dunbar, M. (1964) Geographical distribution of superstructure icing in the northern hemisphere. Report Misc. G-15, Directorate of Physical Research, Defence Research Board, Canada.

Fein, N. and A. Freiberger (1965) Survey of the literature on shipboard ice formation. Tech. Memo. 2, U.S. Naval Applied Science Laboratory, Brooklyn, New York.

Gerger, H. (1974) Methods used to minimize, prevent and remove ice accretion on meteorological surface instruments. Technical Note 135, World Meteorological Organization, Geneva.

Glukhov, V.G. (1971) Evaluation of ice loads on high structures from aerological observations (in Russian). Trudy, vol. 283 GGO, p. 3-11. Leningrad: Gidrometeoizdat. (Translation: Soviet Hydrology; Selected papers, p. 223-8, Issue no. 3, 1971.)

Glukhov, V.G. (1972) Meteorological conditions for formation of ice on high structures (in Russian). Leningrad: Gidrometeoizdat, Trudy, vol. 311, GGO.

Guttman, Nathaniel B. (1971) Study of worldwide occurrence of fog, thunderstorms, supercooled low clouds and freezing temperatures. Naval Weather Service Command, NAVAIR 50-1C-60.

Houghton, H.G. and W.H. Radford (1938) On the measurement of drop size and liquid water content in fogs and clouds. M.I.T. Papers on Physical Oceanography and Meteorology.

Kaplina, T.E. and K.I. Chukanin (1971) Studying synoptic conditions favorable for ship icing. In *Theoretical and experimental studies of ship icing* (in Russian). Leningrad: Gidrometeoizdat, p. 171-175.

Kaplina, T.E. and K.I. Chukanin (1972) Synoptic conditions for particularly severe icing of commercial vessels (in Russian). Leningrad: Arkticheskii i antarkticheskii nauchno-issledovatel'skii institut. Trudy, vol. 298, p. 168-173. Also in CRREL Draft Translation 411, AD A003215.

Kliuchnikova, L.A. (1971) Physical processes causing icing of SRT-type ships. In *Theoretical and experimental studies of ship icing* (in Russian). Leningrad: Gidrometeoizdat, p. 16-25.

Kocmond, W.C., R.J. Pilié, W.J. Eadie, E.J. Mack and R.P. Leonard (1971) Investigation of warm fog properties and fog modification concepts. NASA CR-1731, National Aeronautics and Space Administration, Washington, D.C.

Kolosova, N.V. (1972) Potential ship icing regions of the Chukchi Sea during summer and fall (in Russian). Leningrad: Arkticheskii i antarkticheskii nauchno-issledovatel'skii institut. Trudy, vol. 298, p. 156-167. Also in CRREL Draft Translation 411, AD A003215.

Kultashev, E.N., N.F. Malakhov, V.V. Panov and M.V. Shmidt (1972) Spray icing of SRT and SRTM Fishing Vessels (in Russian). Leningrad: Arkticheskii i antarkticheskii nauchno-issledovatil'skii institut. Trudy, vol. 298, p. 125-136, Also in CRREL Draft Translation 411, AD A003215.

Kuroiwa, D. (1965) Icing and snow accretion on electric wires. CRREL Research Report 123, AD 611750.

Kuznetsov, A.V. (1971) Probability of ship icing in the Kara Sea with various synoptic processes. In *Theoretical and experimental studies of ship icing* (in Russian), Leningrad: Gidrometeoizdat, p. 183-189.

Kuznetsov, V.P., E.N. Kultashev, V.V. Panov, A.P. Tiurin and A.V. Sharapov (1971) Studying ship icing in the sea of Japan in 1969. In *Theoretical and experimental studies of ship icing* (in Russian). Leningrad: Gidrometeoizdat, p. 57-68.

Lai, R.J. and O.H. Shemdin (1974) Laboratory study of the generation of spray over water. *Journal of Geophysical Research*, vol. 79, no. 21, p. 3055-63.

Landy, M. and A. Freiberger (1968) An approach to the shipboard icing problem. *Journal American Society of Naval Engineers*, vol. 80, no. 1, p. 63-72.

Langmuir, I. and K. Blodgett (1946) Mathematical investigation of water droplet trajectories. U.S. Army Air Force Technical Report 5418.

Mertins, H.O. (1968) Icing on fishing vessels due to spray. *Marine Observer*, vol. 38, no. 221, p. 128-30.

National Aeronautics and Space Administration (1968) Marine climatic guide. Prepared by Spaceflight Meteorology Group for Manned Spacecraft Center, Houston, Texas.

Panov, V.V. (1971) Calculation of the quantity of ice accumulating on ships during spray icing. In *Theoretical and experimental studies of ship icing* (in Russian). Leningrad: Gidrometeoizdat, p. 26-48.

Panov, V.V. (1971a) Frequency and degree of spraying of the SRT-type ships. In *Theoretical and experimental studies of ship icing* (in Russian). Leningrad: Gidrometeoizdat, p. 87-90.

Panov, V.V. (1972) Water drop temperature and ice salinity calculations related to icing of ships from spray (in Russian). Leningrad: Arkticheskii i antarkticheskii nauchno-issledovatel'skii institut, Trudy, vol. 298, p. 44-50. Also in CRREL Draft Translation 411, AD A003215.

Panov, V.V. and M.V. Shmidt (1971) Gradations of hydrometeorological complexes of icing, considering their danger to ships, *Problemy Arktiki i Antarktiki*, vol. 38, p. 120-124 (translation by American Publishing Co. Ltd., New Delhi).

Pilié, R.J. and W.C. Kocmond (1967) Project fog drops. Cornell Aeronautical Laboratory. NASA CR-675, National Aeronautics and Space Administration, Washington, D.C.
Polar Record (1958) Research on anti-icing precautions for ships. vol. 9, no. 58, p. 36-9.
Rubin, E.H. (1969) Ice accretion studies under simulated shipboard icing conditions. Final Report, Project 930-20, U.S. Naval Applied Science Laboratory, Brooklyn, New York.
Sharapov. A.V. (1971a) Intensity of icing of small SRT ships. In *Theoretical and experimental studies of ship icing* (in Russian). Leningrad: Gidrometeoizdat, p. 95-97.
Sharapov, A.V. (1971b) Quantity of water brought to the SRT ships by sea spray. In *Theoretical and experimental studies of ship icing* (in Russian). Leningrad: Gidrometeoizdat, p. 91-94.
Shekhtman, A.N. (1967) Hydrometeorological conditions of ship icing (in Russian). Moscow: Nauchno-issledovatel' skii institut aeroklimatologii. Trudy, vol. 45, p. 51-63. Also, Translation by Naval Research and Development Adminstration, Ministry of Defence, United Kingdom.
Shekhtman, A.N. (1968) The probability and intensity of the icing-up of ocean-going vessels (in Russian). Moscow: Nauchno-issledovatel'skii institut aeroklimatologii. Trudy, vol. 50, p. 55-65.
Shellard, H.C. (1974) The meteorological aspects of ice accretion on ships. Marine Science Affairs Report no. 10 (WMO-No. 397), World Meteorological Organization, Geneva.
Smirnov, V.I. (1972) Fighting ship icing conditions (according to foreign data) (in Russian). Leningrad: Arkticheskii i antarkticheskii nauchno-issledovatel'skii institut. Trudy, vol. 298, p. 174-178. Also in CRREL Draft Translation 411, AD A003215.
Stallabrass, J.R. (1970) Methods for the alleviation of ship icing. Mechanical Engineering Report MD-51, National Research Council, Ottawa, Canada.
Stallabrass, J.R. (1971) Meteorological and oceanographic aspects of trawler icing off the Canadian east coast. *Marine Observer*, vol. 41, no. 233, p. 107-121.
Stallabrass, J.R. and P.F. Hearty (1967) The icing of cylinders in conditions of simulated freezing sea spray. Mechanical Engineering Report MD-50, NRC no. 9782, National Research Council, Ottawa, Canada.
Tabata, T. (1968) Research on prevention of ship icing. Report to Hokkaido Prefectural Government, Translation no. T95J, Defence Research Board, Ottawa, Canada.
Tabata, T., S. Iwata and N. Ono (1963) Studies on the ice accumulation on ships. I. *Low Temperature Science*, series A, vol. 21, p. 173-221.
U.S. Navy (1958) Oceanographic atlas of the polar seas. Part II, Arctic. U.S. Navy Hydrographic Office, Pub. No. 705, Washington, D.C.
U.S. Navy (1963) Marine climatic atlas of the world. vol. VI, (NAVWEPS 50-1C-533), U.S. Government Printing Office, Washington, D.C.
Vasil'eva, G.V. (1967) Hydrometeorological conditions causing ice accretion on ships. Translation T486R, Defence Research Board, Ottawa, Canada. Translated from *Rybnoye Khoziaistvo* (1966), vol. 12, p. 43-45.
Vasil'eva, G.V. (1971) Cases of ship icing in the Far East in January 1968. In *Theoretical and experimental studies of ship icing* (in Russian). Leningrad: Gidrometeoizdat, p. 166-170.
Weickmann, H.K. and H.J. aufm Kampe (1953) Physical properties of cumulus clouds. *Journal of Meteorology*, vol. 10, p. 204.
Woodcock, A.H. (1953) Salt nuclei in marine air as function of altitude and wind force. *Journal of Meteorology*, vol. 10, no. 5, p. 362-71.
Wu, J. (1973) Spray in the atmospheric surface layer: Laboratory study. *Journal of Geophysical Research*, vol. 78, no. 3, p. 511-19.
Yerokhin, Ye. (1968) Safe navigation during icing of ships. *Morskoi Flot*, vol. 21, no. 9, p. 15-18. (Also Translation no. T485R, Defence Research Board, Ottawa, Canada.)

APPENDIX A. MAPS OF ICING OCCURRENCE AND RATE

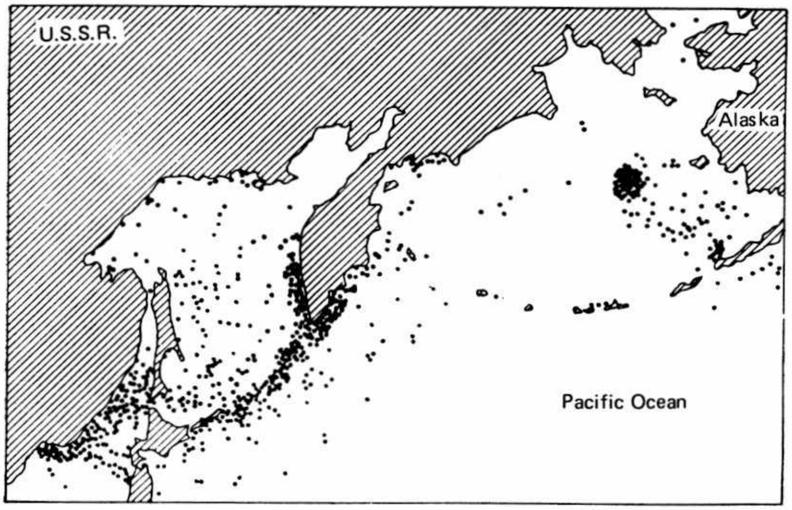

Figure A1. Locations of reported ship icing in the North Pacific Ocean and the Far East (Borisenkov and Panov 1972).

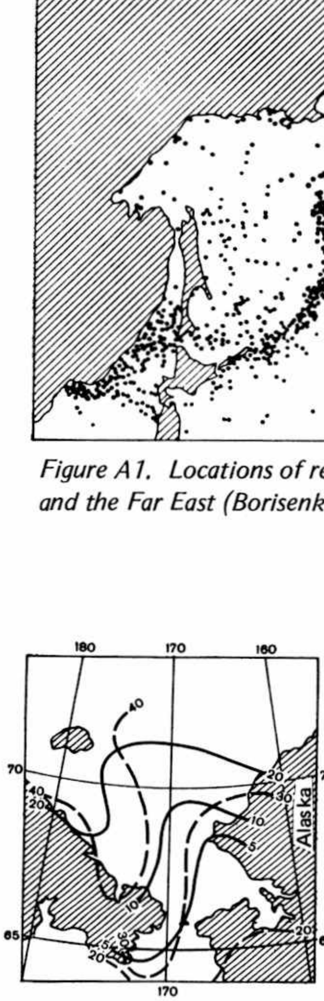

Figure A2. Probability (in percentage) of meteorological conditions conducive to the development of spray icing (combination of $t_a \leq 0°C$ and $V \geq 8$ m/s) in September (—) and October (- - -), from Kolosova (1972).

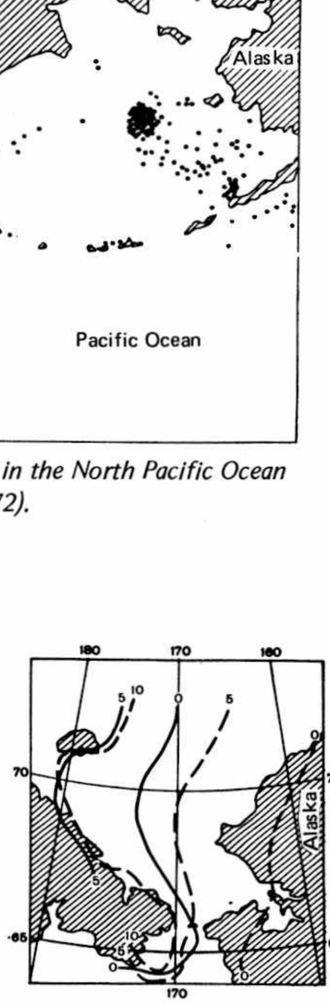

Figure A3. Probability (in percentage) of meteorological conditions conducive to the development of dangerous spray icing (combination of $t_a < 0°C$ and $V >> 15$ m/s) in September (—) and October (- - -), from Kolosova (1972).

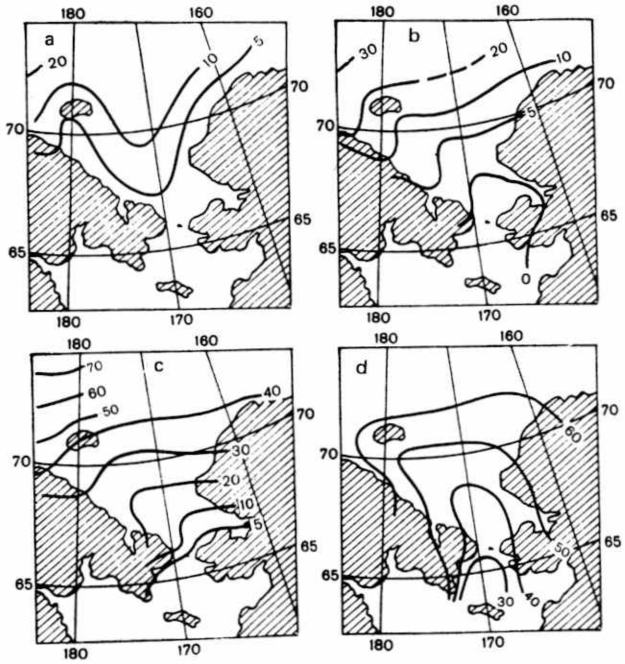

Figure A4. Probability (in percentage) of meteorological conditions conducive to the development of freshwater icing (combination of $t_a \leq 0°C$ and $V \leq 7\ m/s$) where a – July, b – August, c – September, and d – October (Kolosova 1972).

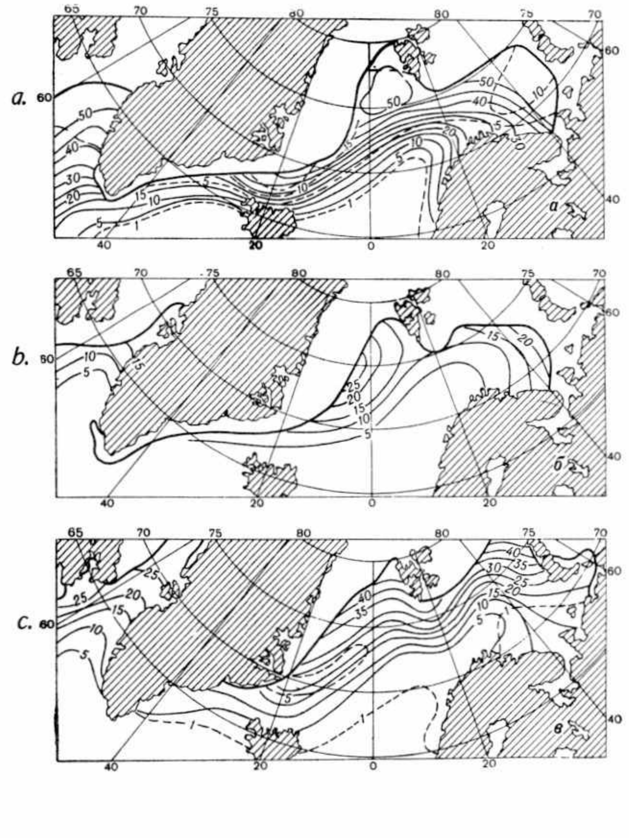

Figure A5. Probability of ship icing: a – February; b – May (spring); c – November (fall). Solid heavy line represents the approximate boundary of continuous ice; solid thin lines the probabilities of hull icing with wind speed greater than 16 knots and air temperature below −1.7°C; broken thin lines are the probabilities of superstructure icing with wind speeds greater than 17 knots and air temperatures below −2.2°C (Smirnov 1972).

POTENTIAL SUPERSTRUCTURE ICING
Moderate (——) Air Temperatures < −2°c, Wind ≥ 13kt
Severe (– – –) Air Temperatures < −9°C, Wind ≥ 30kt

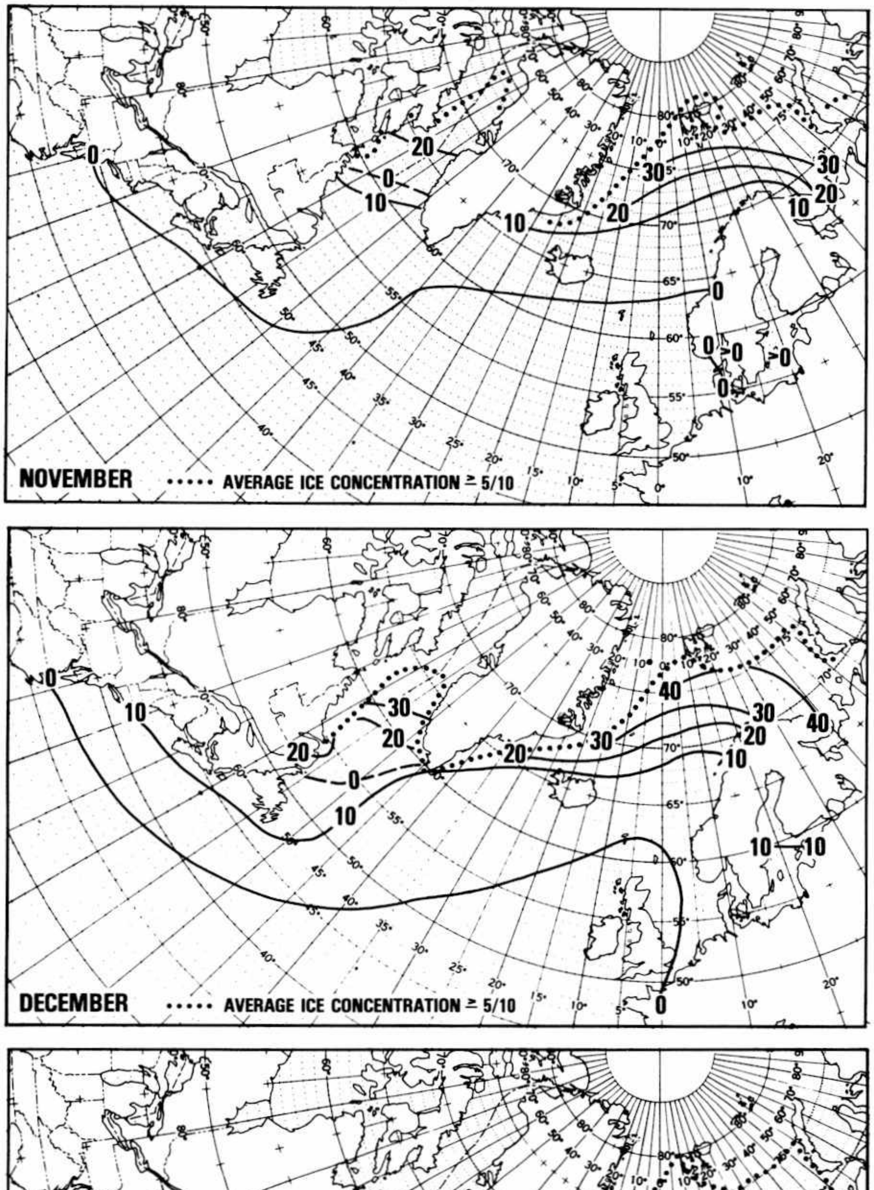

Figure A6. Moderate and severe potential superstructure icing for Nortn Atlantic; November–January (DeAngelis 1974).

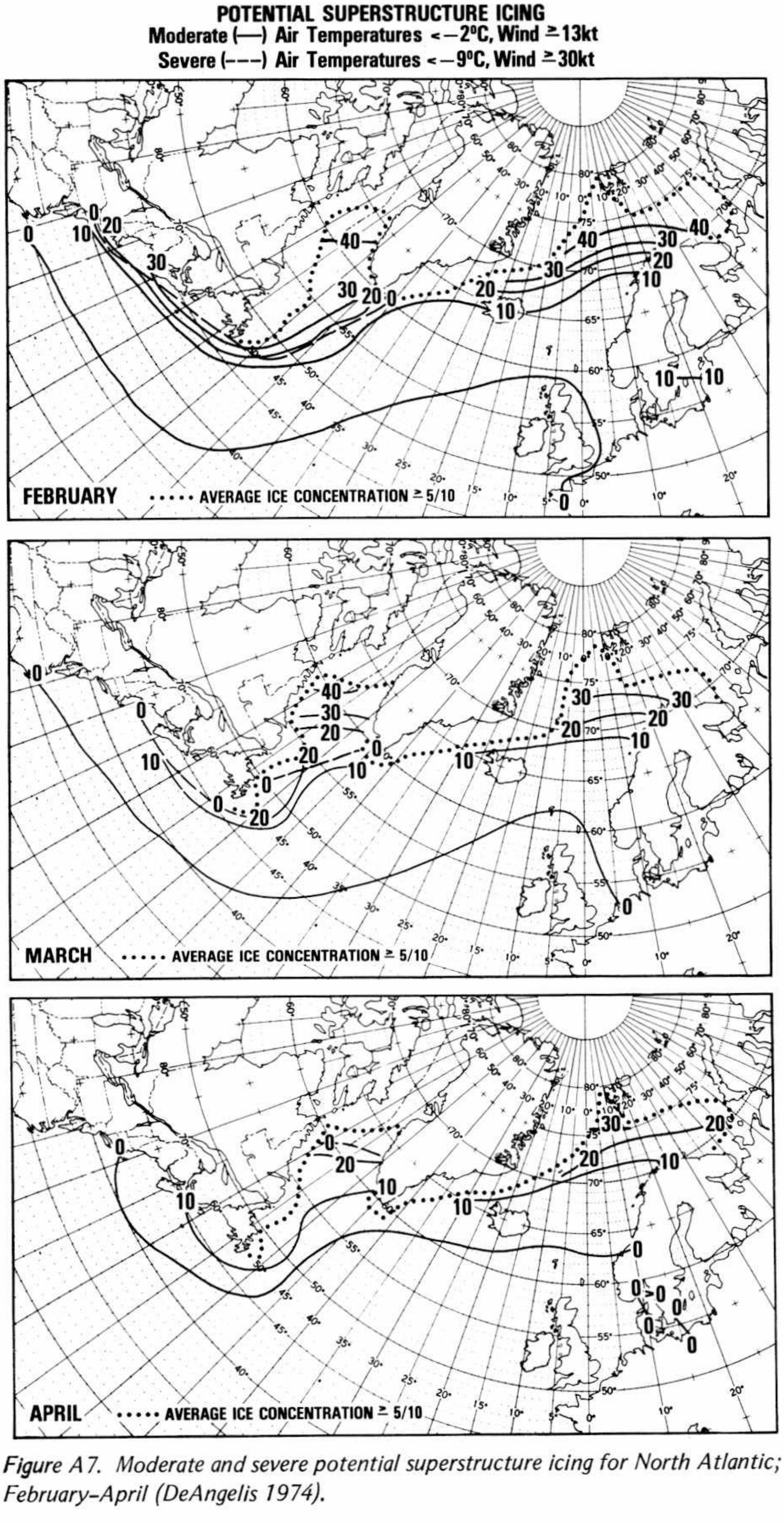

Figure A7. Moderate and severe potential superstructure icing for North Atlantic; February–April (DeAngelis 1974).

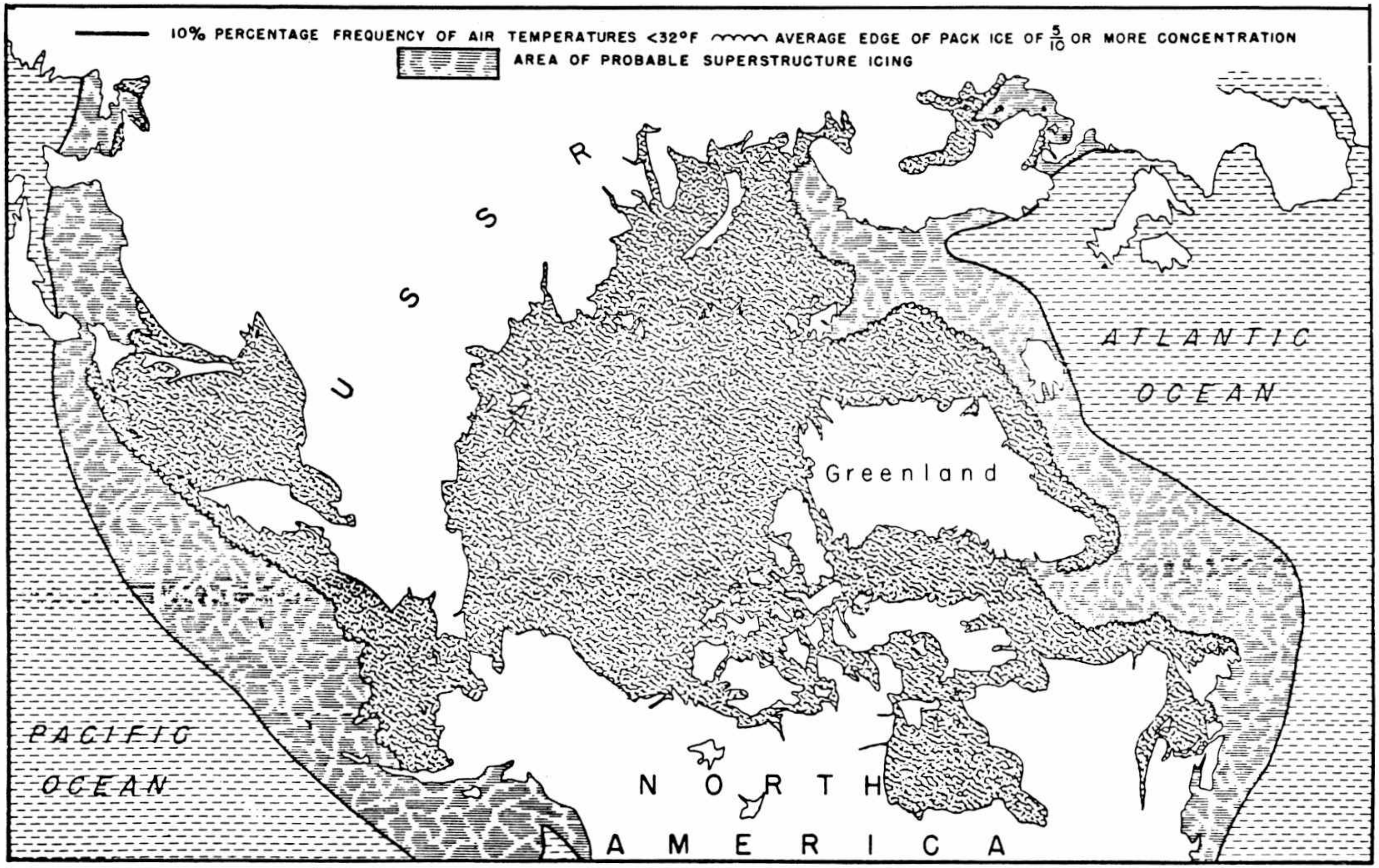

a. January–March.

Figure A8. Probability of superstructure icing (Dunbar 1964).

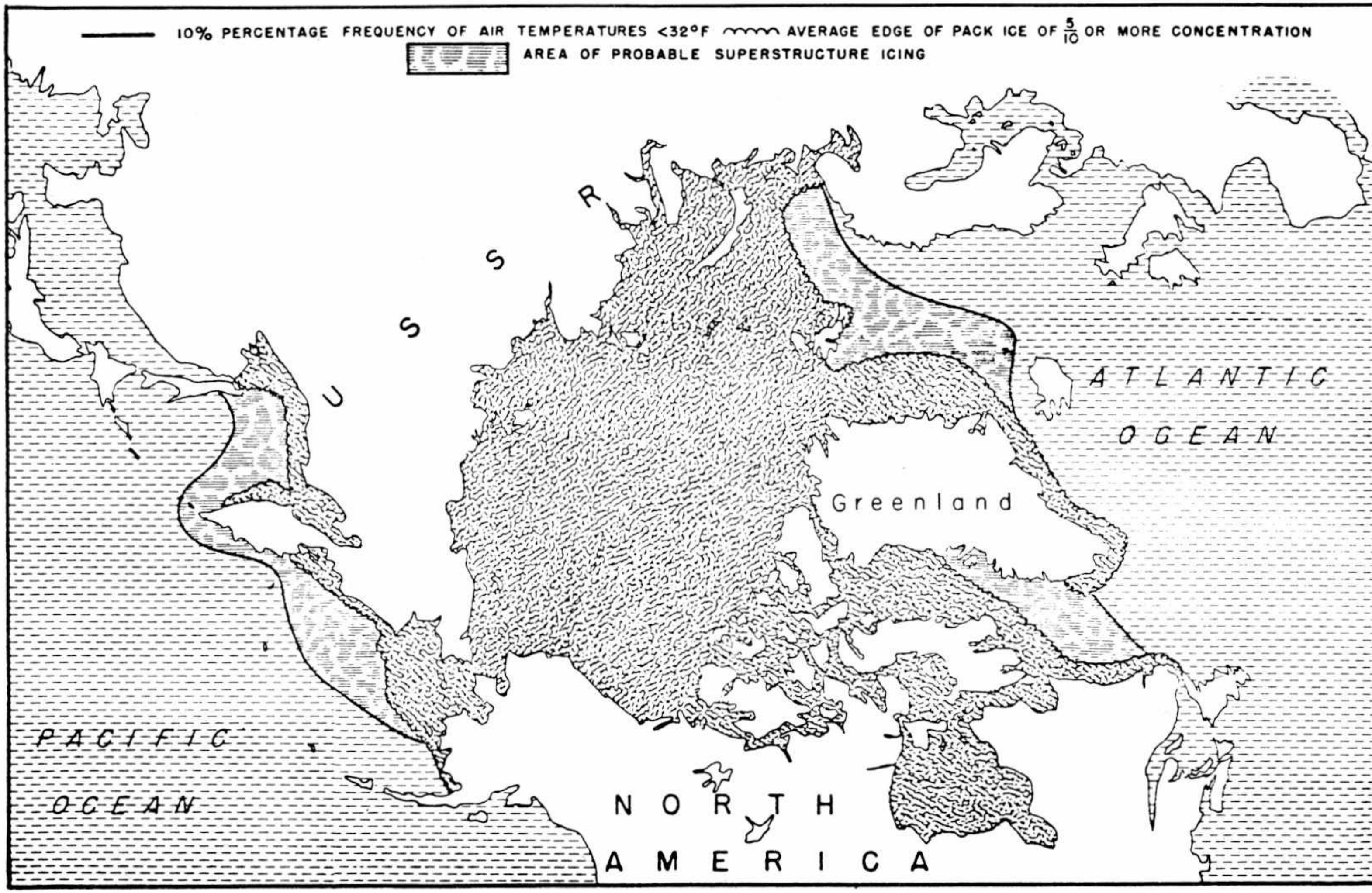

b. May.

Figure A8 (cont'd). Probability of superstructure icing (Dunbar 1964).

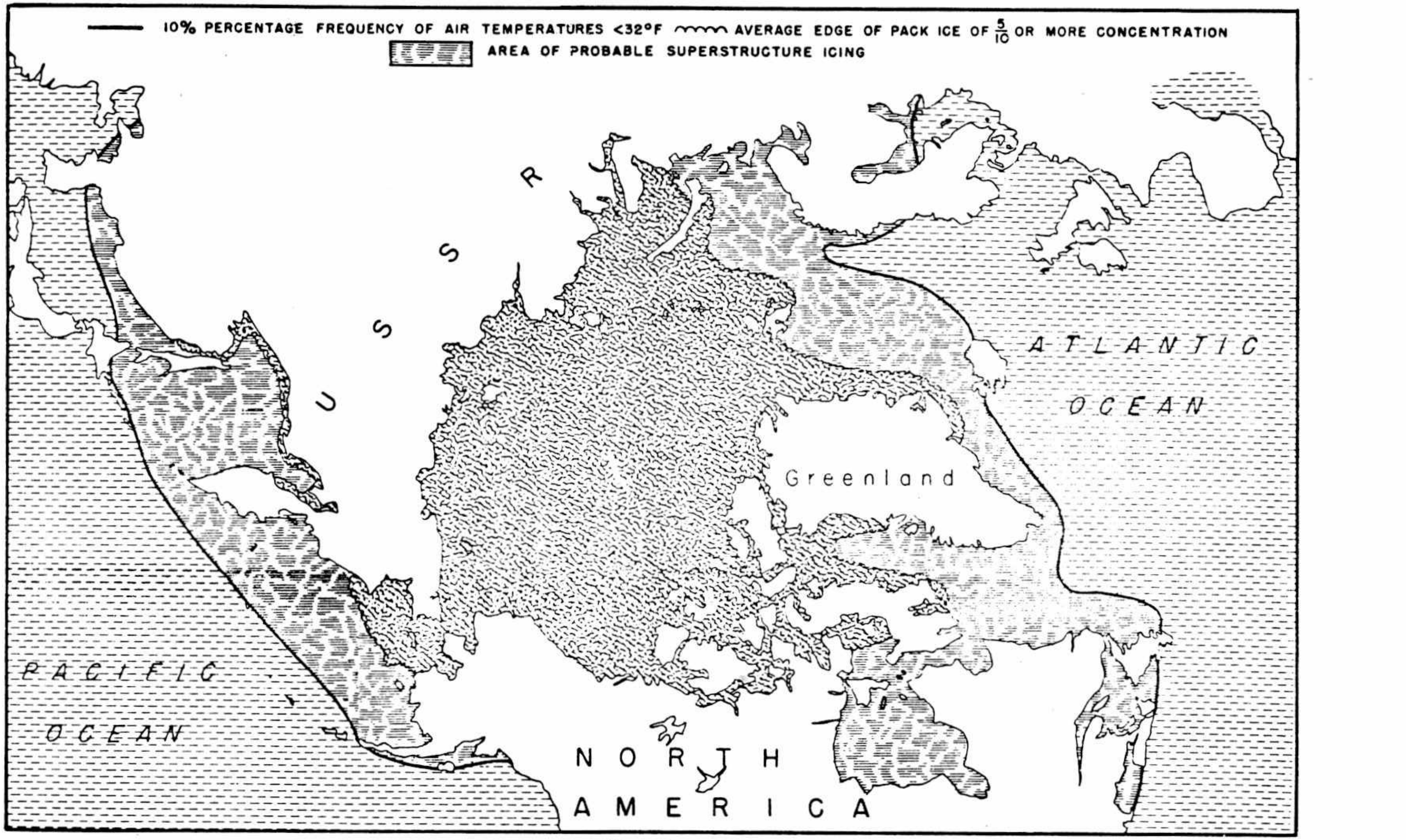

c. November.

Figure A8 (cont'd).

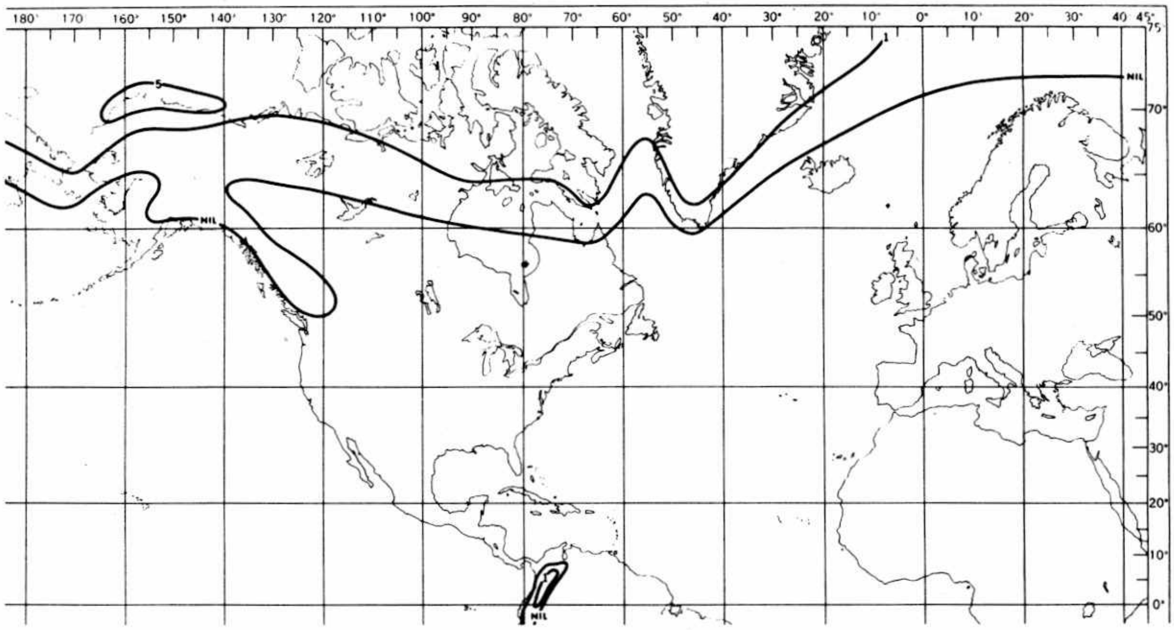

a. September.

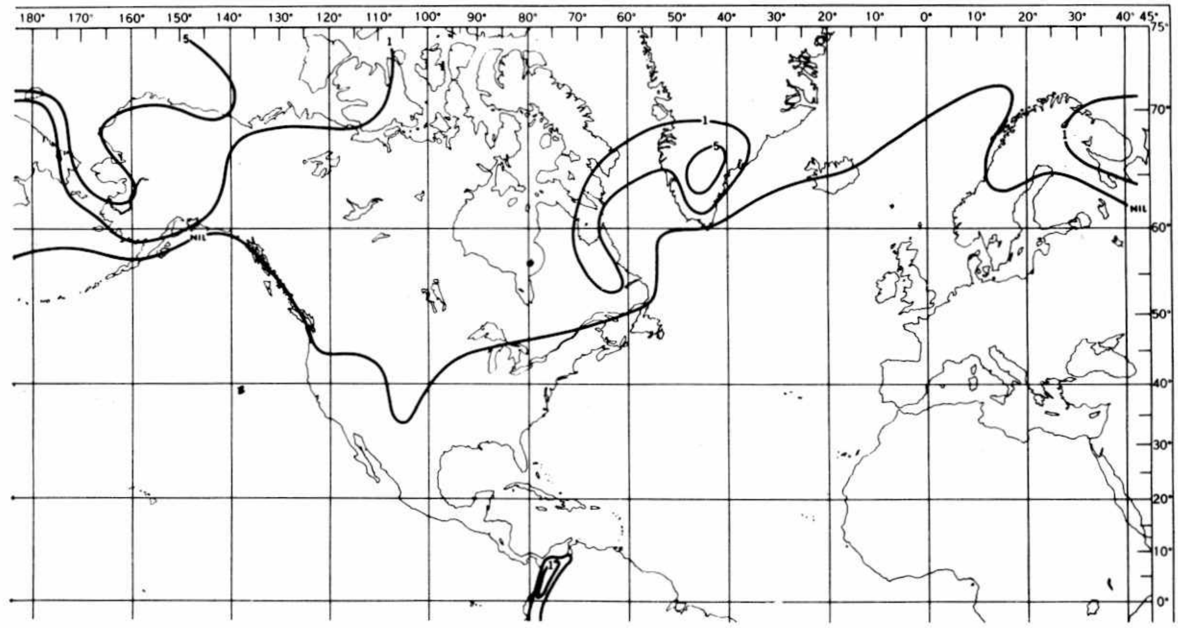

b. October.

Figure A9. Probability of occurrence of supercooled fog (%) by month (Guttman 1971).

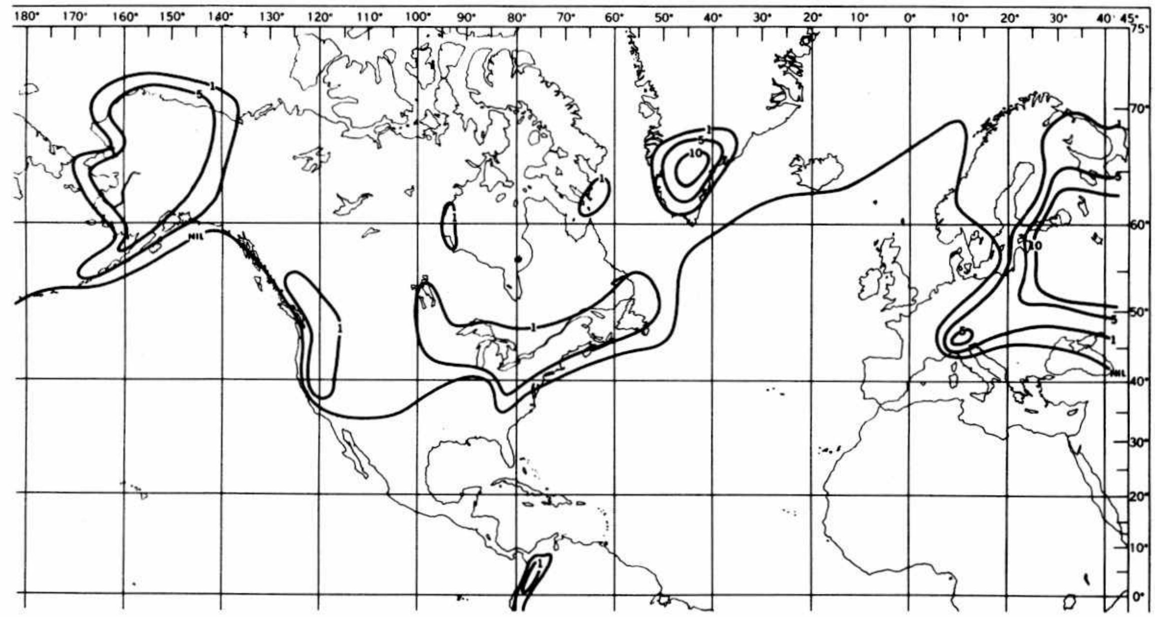

c. November.

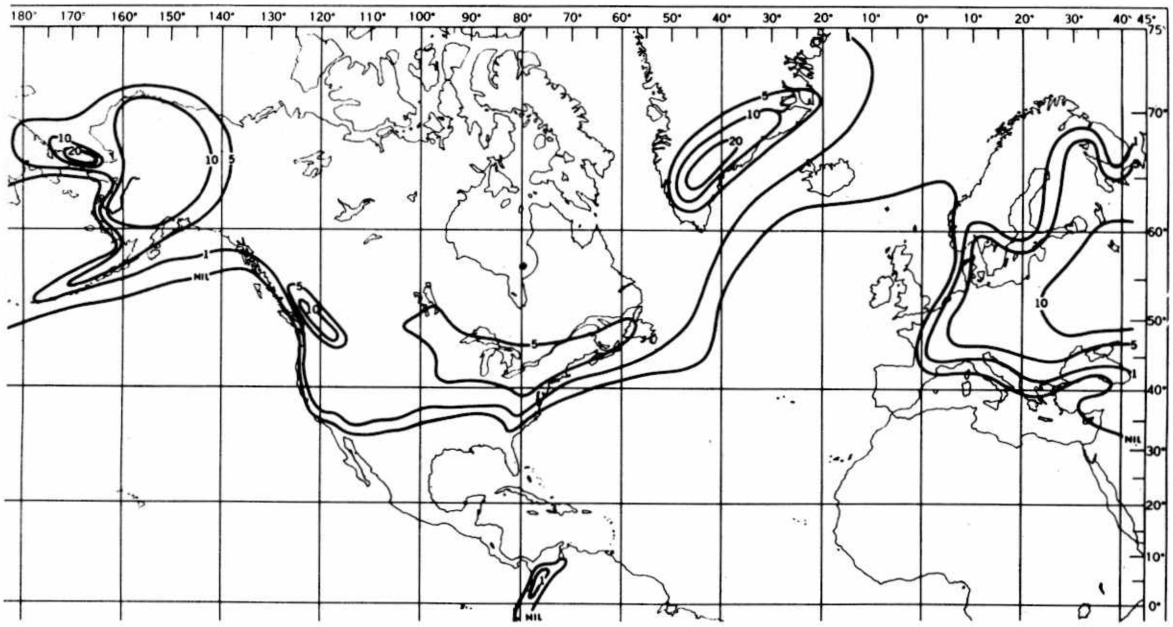

d. December.

Figure A9 (cont'd).

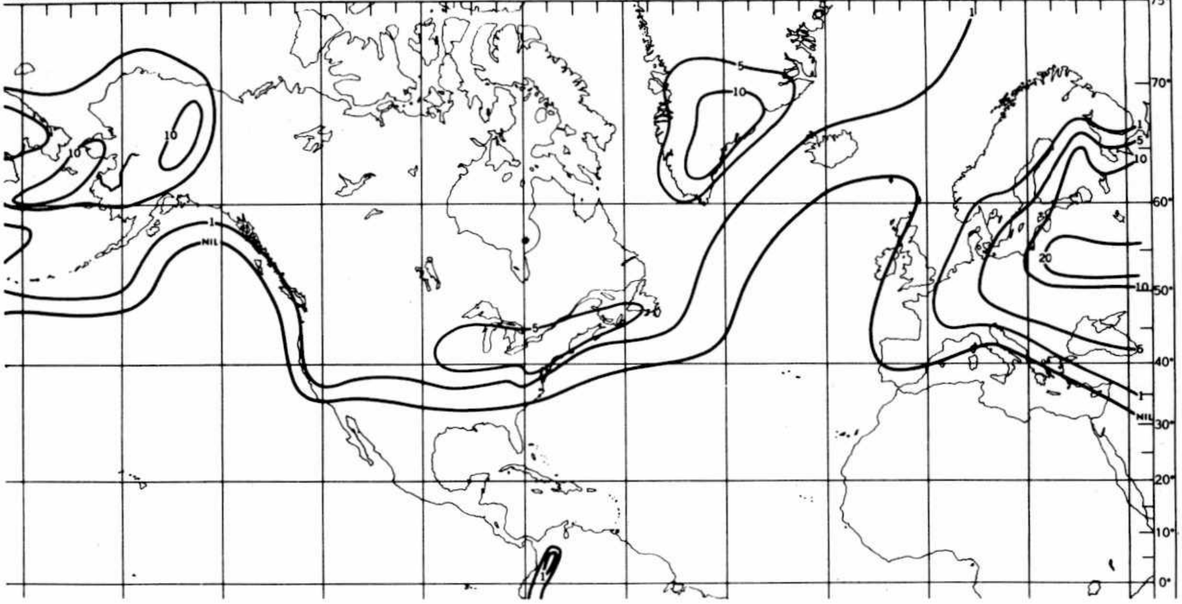

e. January.

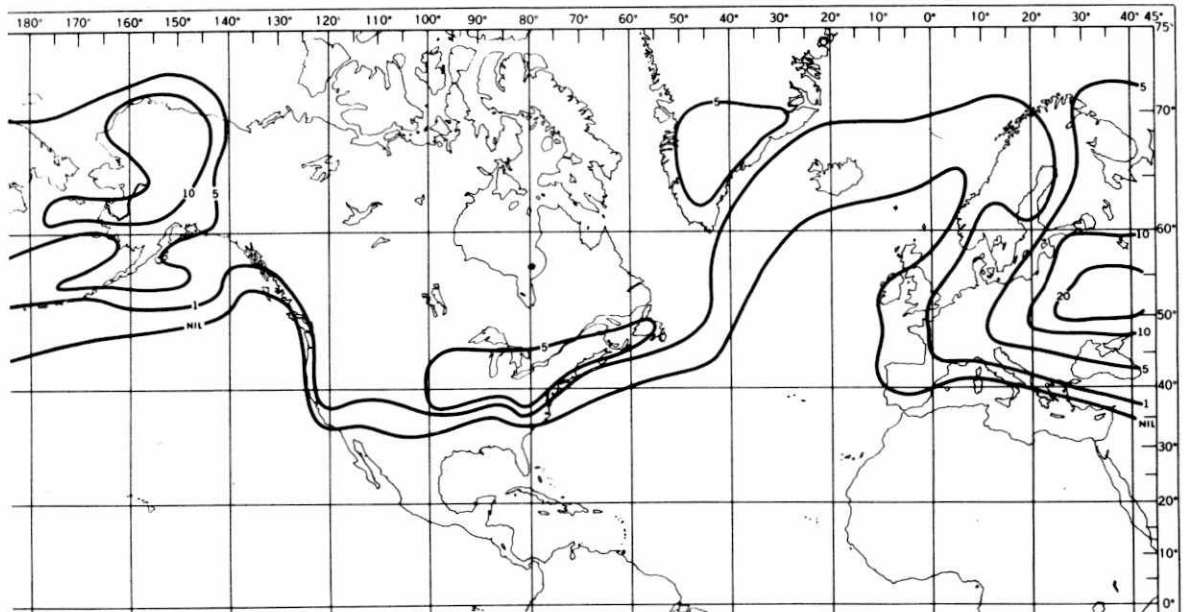

f. February.

Figure A9 (cont'd). Probability of occurrence of supercooled fog (%) by month (Guttman 1971).

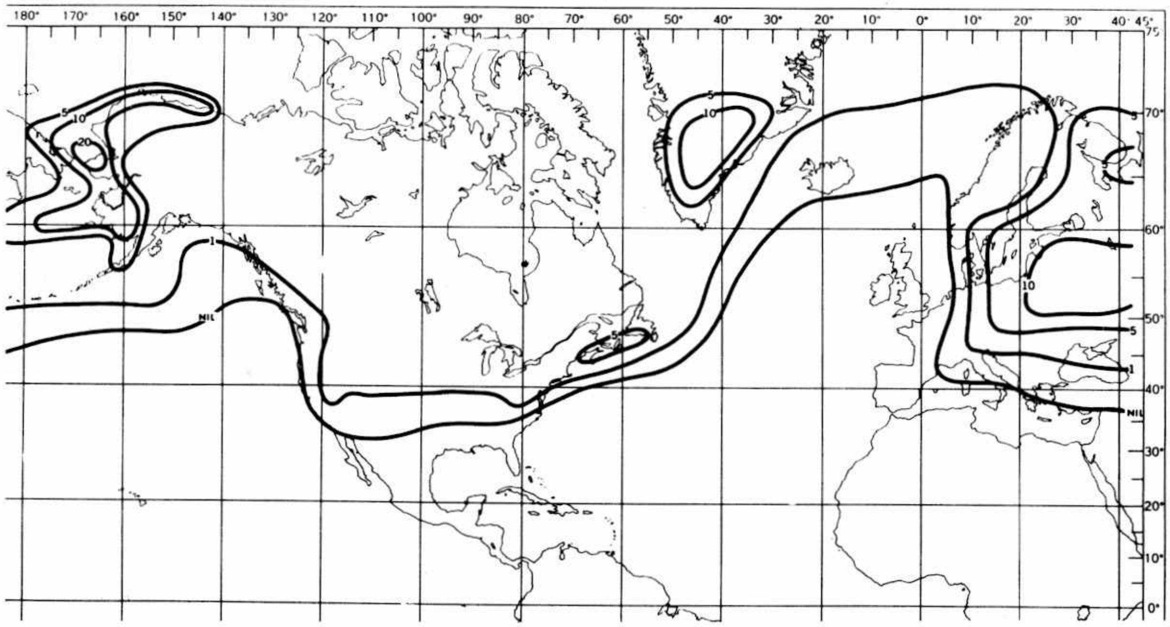

g. March.

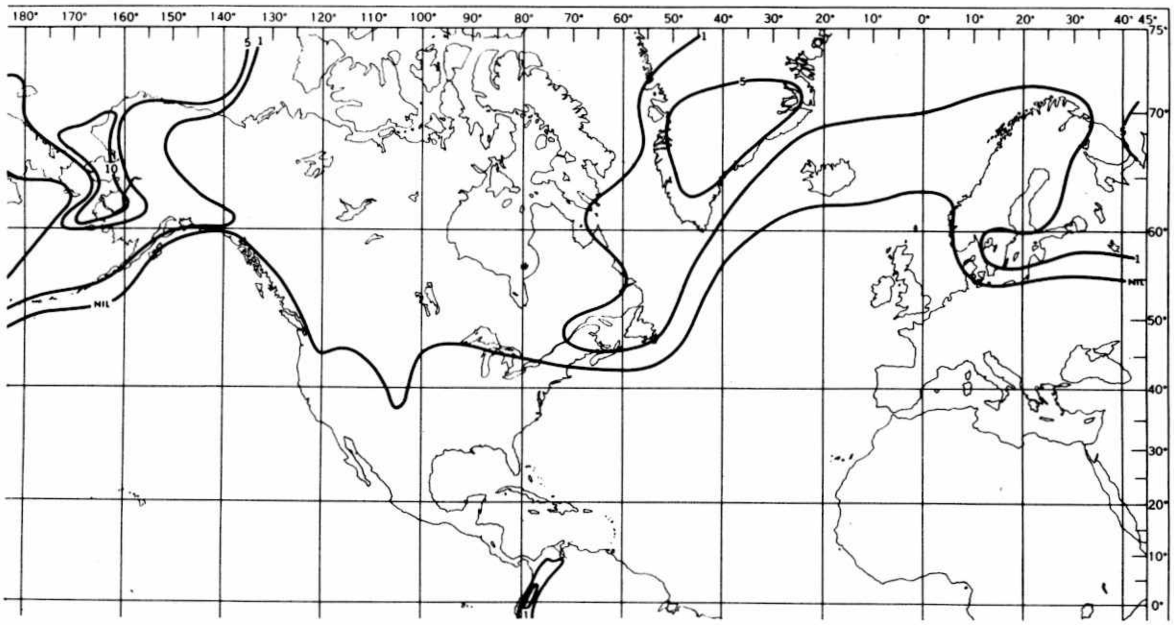

h. April.

Figure A9.(cont'd).

APPENDIX B. DATA FOR COMPUTING SHIP ICING RATES

Table BI. Effective heat of fusion (cal/g) of fresh-water and sea ice (Borisenkov and Pchelko 1972).

T_ℓ (°C)	Salinity (°/₀₀) 0	5	10	15	20	25	30	35
− 1	80.12	59.09	37.98	16.87				
− 2	80.62	69.60	58.53	47.45	36.36	25.28	14.19	3.11
− 3	81.13	73.57	66.95	58.32	50.70	43.07	35.44	30.92
− 5	82.14	77.39	72.58	67.77	62.96	58.14	58.32	48.51
− 8	83.66	80.42	77.13	73.83	70.54	67.23	63.94	60.63
−10	84.66	81.92	79.12	76.31	73.51	70.70	67.89	65.08
−15	87.18	85.04	82.85	80.66	78.46	76.25	74.05	71.84
−20	89.70	87.96	86.21	84.42	82.64	80.85	79.06	77.28
−23	91.21	89.84	88.42	86.99	85.56	84.13	82.69	81.25
−25	92.22	91.21	90.13	89.06	87.98	86.90	85.81	84.72
−30	94.74	93.94	93.09	92.24	91.37	90.50	89.63	88.76

Table BII. Effective heat capacity (cal/g °C) of fresh-water ice and sea ice at various temperatures and salinities (Borisenkov and Pchelko 1972).

T_ℓ (°C)	Salinity (°/₀₀) 0	5	10	15	20	25	30	35
− 1	0.502	20.373	40.245	60.115				
− 2	0.501	5.646	10.792	15.938	21.084	26.229	31.374	36.519
− 3	0.499	2.837	5.176	6.513	9.852	12.191	14.540	16.868
− 5	0.495	1.337	2.176	3.021	3.862	4.704	5.546	6.388
− 8	0.490	0.801	1.113	1.424	1.736	2.047	2.357	2.670
−10	0.486	0.679	0.871	1.064	1.257	1.450	1.642	1.835
−15	0.477	0.572	0.665	0.760	0.855	0.948	1.043	1.138
−20	0.468	0.538	0.609	0.679	0.750	0.820	0.890	0.960
−23	0.463	0.733	1.003	1.273	1.545	1.816	2.087	2.358
−25	0.459	0.551	0.643	0.735	0.826	0.919	1.010	1.101
−30	0.450	0.469	0.488	0.507	0.526	0.545	0.563	0.581

Table BIII. Heat capacity *C* of fresh and sea water (cal/g °C) at standard atmospheric pressure as a function of temperature and salinity (Borisenkov and Pchelko 1972).

T_ℓ (°C)	Salinity (°/₀₀)								
	0	5	10	15	20	25	30	35	40
3	1.003	0.995	0.987	0.980	0.972	0.965	0.959	0.952	0.945
2	1.005	0.997	0.988	0.980	0.973	0.965	0.958	0.952	0.945
1	1.006	0.997	0.989	0.981	0.973	0.965	0.958	0.952	0.945
0	1.007	0.998	0.989	0.981	0.973	0.965	0.958	0.952	0.945
−1					0.973	0.965	0.958	0.951	0.945
−2								0.951	0.945

Table BIV. Temperature of 2.4-mm water drop as a function of air temperature and flight time (Borisenkov and Pchelko 1972, Panov 1972).

Flight time of droplet (s)	Air temperature (°C)						
	0	−2	−5	−10	−15	−20	−30
				Initial water temperature −1.7°			
1	−1.42	−1.75	−2.24	−3.07	− 3.89	− 4.72	− 6.37
2	−1.19	−1.79	−2.70	−4.21	− 5.72	− 8.23	−10.25
3	−0.99	−1.83	−3.08	−5.16	− 7.25	− 9.33	−13.50
4	−0.83	−1.85	−3.39	−5.96	− 8.52	−11.09	−16.22
5	−0.69	−1.88	−3.66	−6.62	− 9.79	−12.55	−17.48
10	−0.28	−1.95	−4.46	−8.63	−12.81	−16.98	−23.35
				Initial water temperature 0°			
1	0	−0.31	−0.78	−1.56	− 2.34	− 3.12	− 4.68
2	0	−0.58	−1.44	−2.88	− 4.32	− 5.76	− 8.64
3	0	−0.80	−2.00	−3.99	− 5.98	− 7.98	−11.97
4	0	−0.98	−2.46	−4.97	− 7.39	− 9.86	−14.79
5	0	−1.15	−2.86	−5.73	− 8.59	−11.46	−17.19
10	0	−1.63	−4.08	−8.17	−12.25	−16.34	−24.51
				Initial water temperature 2°			
1	1.69	1.38	0.91	0.13	− 0.65	− 1.44	− 2.09
2	1.42	0.85	−0.02	−1.46	− 2.90	− 4.34	− 7.22
3	1.20	0.40	−0.79	−2.79	− 4.78	− 6.78	−10.77
4	1.01	−0.03	−1.45	−3.92	− 6.38	− 8.85	−13.78
5	0.85	−0.29	−2.11	−4.88	− 7.74	−10.61	−16.54
10	0.37	−1.27	−3.72	−7.80	−11.89	−15.97	−24.43

Table BV. Temperature of 1-mm water drop as a function of air temperature and flight time (Panov 1972).

Flight time of droplet (s)	Air temperature (°C) 0	−2	−5	−10	−15	−20	−30
				Initial water temperature −1.7°			
1	−1.68	−1.70	−1.73	−1.78	−1.83	−1.88	−1.98
2	−1.65	−1.71	−1.80	−1.95	−2.10	−2.25	−2.55
3	−1.63	−1.71	−1.83	−2.03	−2.22	−2.41	−2.28
4	−1.60	−1.72	−1.89	−2.18	−2.47	−2.76	−3.34
5	−1.58	−1.72	−1.92	−2.26	−2.60	−2.94	−3.62
10	−1.46	−1.74	−2.16	−2.85	−3.55	−4.24	−5.63
				Initial water temperature 0°			
1	0	−0.02	−0.05	−0.10	−0.15	−0.20	−0.30
2	0	−0.06	−0.15	−0.30	−0.45	−0.60	−0.90
3	0	−0.08	−0.19	−0.39	−0.58	−0.78	−1.17
4	0	−0.12	−0.29	−0.58	−0.87	−1.16	−1.74
5	0	−0.14	−0.34	−0.68	−1.02	−1.36	−2.04
10	0	−0.28	−0.69	−1.39	−2.08	−2.78	−4.17
				Initial water temperature 2°			
1	1.98	1.96	1.93	1.88	1.83	1.76	1.68
2	1.94	1.88	1.79	1.64	1.49	1.34	1.04
3	1.92	1.84	1.73	1.53	1.34	1.14	0.75
4	1.88	1.77	1.59	1.30	1.01	0.72	0.14
5	1.86	1.73	1.52	1.18	0.84	0.50	−0.18
10	1.72	1.41	1.08	0.33	−0.36	−1.06	−2.45

Table BVI. Saturated water vapor pressure above water (mbar), from Borisenkov and Pchelko (1972).

T_a (°C)	0°	1°	2°	3°	4°	5°	6°	7°	8°	9°
−30	0.51	0.46	0.42	0.38	0.35	0.31	0.28	0.26	0.23	0.21
−20	1.25	1.15	1.06	0.96	0.88	0.81	0.74	0.67	0.61	0.56
−10	2.86	2.64	2.44	2.25	2.08	1.91	1.76	1.62	1.49	1.37
0	6.11	5.68	5.27	4.90	4.55	4.21	3.91	3.62	3.35	3.10

Table BVII. Saturated water vapor pressure above ice (mbar), from Borisenkov and Pchelko (1972).

T_ℓ (°C)	0°	1°	2°	3°	4°	5°	6°	7°	8°	9°
0	6.11	5.62	5.17	4.76	4.37	4.02	3.68	3.38	3.10	2.84
−10	2.60	2.38	2.17	1.96	1.81	1.65	1.51	1.37	1.25	1.14
−20	1.08	0.94	0.85	0.77	0.70	0.63	0.57	0.52	0.47	0.42
−30	0.38	0.34	0.31	0.28	0.25	0.22	0.20	0.18	0.16	0.14

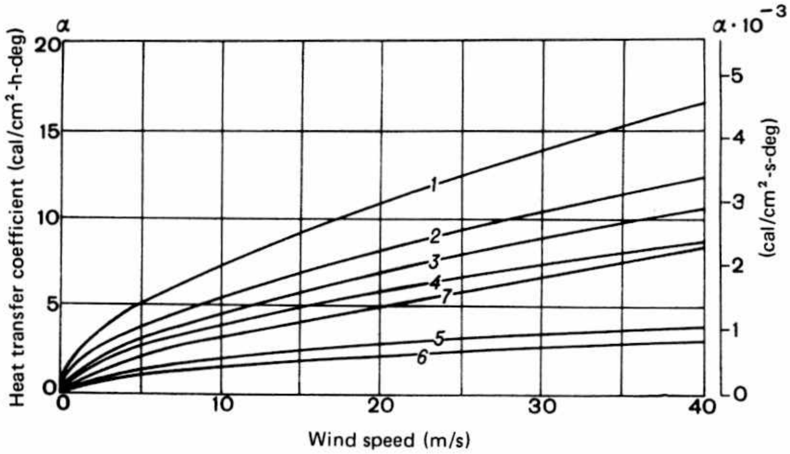

Figure B1. Heat transfer coefficient of cylindrical structures on ships vs apparent wind speed (Borisenkov and Pchelko 1972). The structure diameters are (1) 1 cm, (2) 2 cm, (3) 3 cm, (4) 5 cm, (5) 30 cm, (6) 50 cm, (7) flat surface.

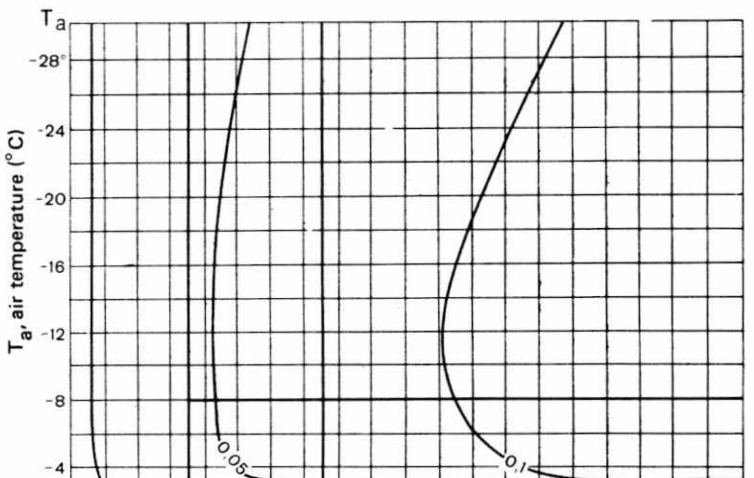

Figure B2. Amount of ice (g/h) which may form on a 1-cm² flat surface during ship icing under the following conditions: $T_a - T_z = 1°C$, $T_a = T_\ell$, $S = 0$ ‰, $L_z = 80.6 - 94.7$, $L_i = 677$, $C_\ell = 0.50 - 0.46$, $C_w = 1.007$ *(Borisenkov et al. 1971).*

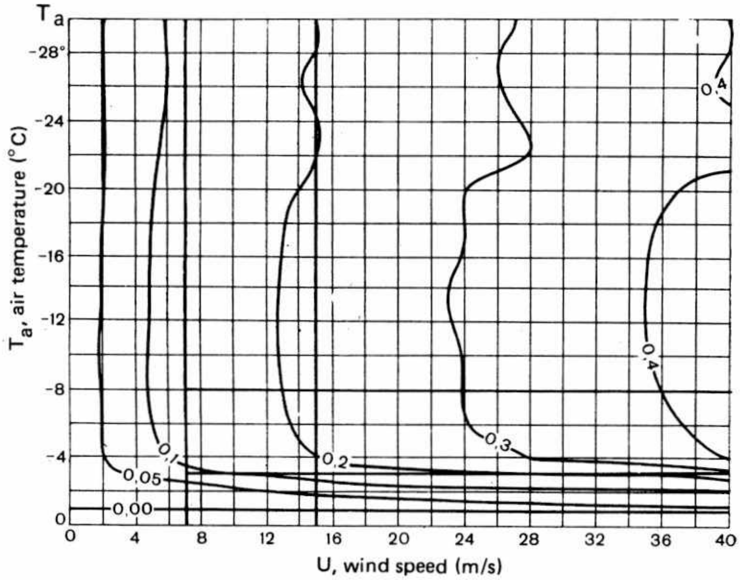

Figure B3. Amount of ice (g/h) which may form on a 1-cm² flat surface during ship icing under the following conditions: $T_a - T_z = 2°C$, $T_a = T_\ell$, $S = 15\,‰$, $L_z = 45.0$, $L_i = 646 - 700$, $C_\ell = 0.7 - 18.0$, $C_w = 0.98$ (Borisenkov et al. 1971).

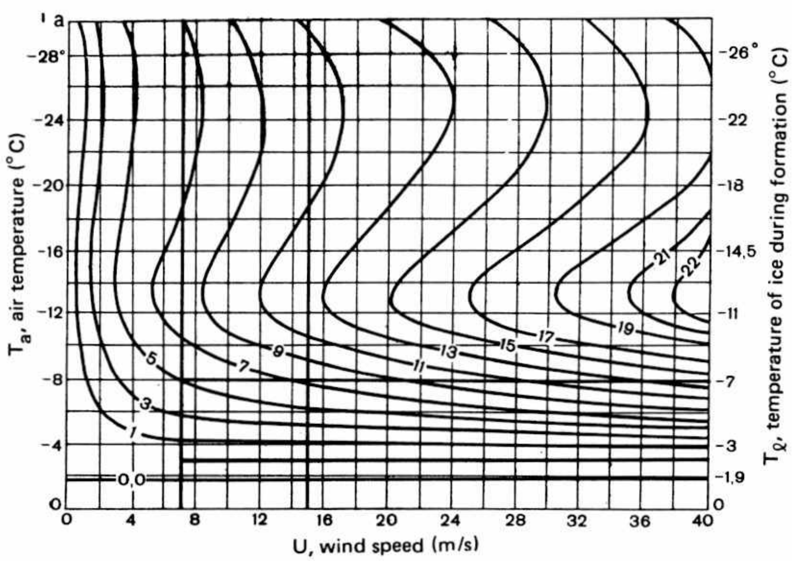

Figure B4. Amount of ice (g/h) which may form on a 1-cm² surface of a 1-cm-diam cylinder during ship icing under the following conditions: $T_w = -1.7°C$, $S = 34\,‰$, $L_z = 4.0$, $L_i = 601 - 700$, $C_\ell = 0.6 - 36.5$, $C_w = 0.96$ (Borisenkov et al. 1971).

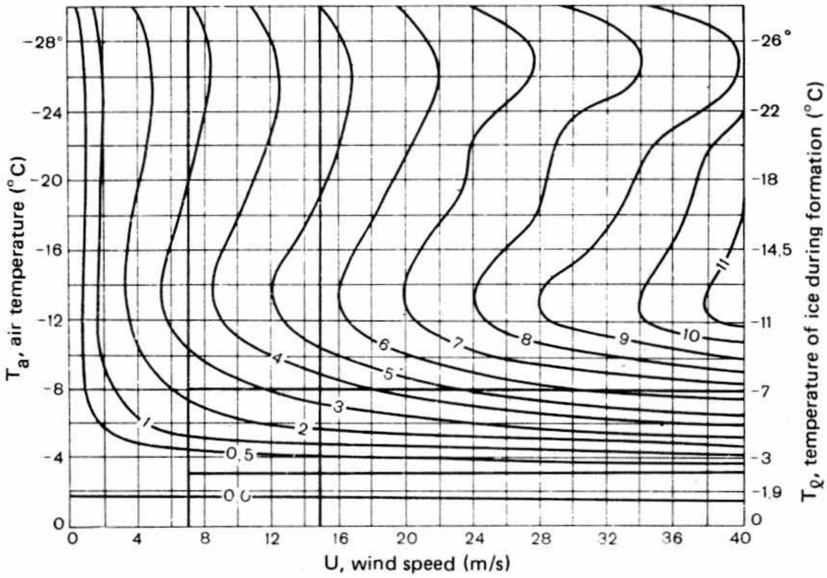

Figure B5. Amount of ice (g/h) which may form on a 1-cm² flat surface during ship icing under the following conditions: $T_w = -1.7°C$, $S = 34\ ^0/_{00}$, $L_z = 4.0$, $L_i = 601 - 700$, $C_\ell = 0.6 - 36.5$, $C_w = 0.96$ (Borisenkov et al. 1971).

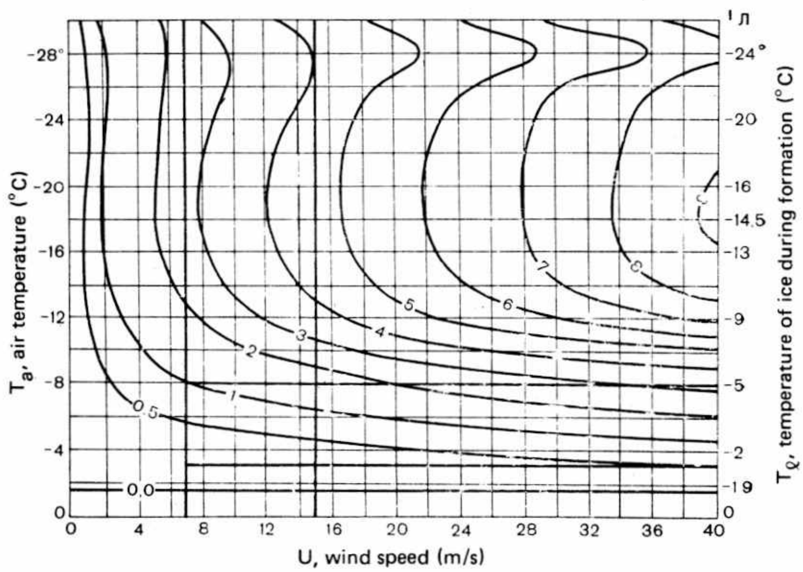

Figure B6. Amount of ice (g/h) which may form on a 1-cm² flat surface during ship icing under the following conditions: $T_w = 1.7°C$, $S = 34\ ^0/_{00}$, $L_z = 4.0$, $L_i = 601 - 700$, $C_\ell = 1.0 - 36.5$, $C_w = 0.96$ (Borisenkov et al. 1971).

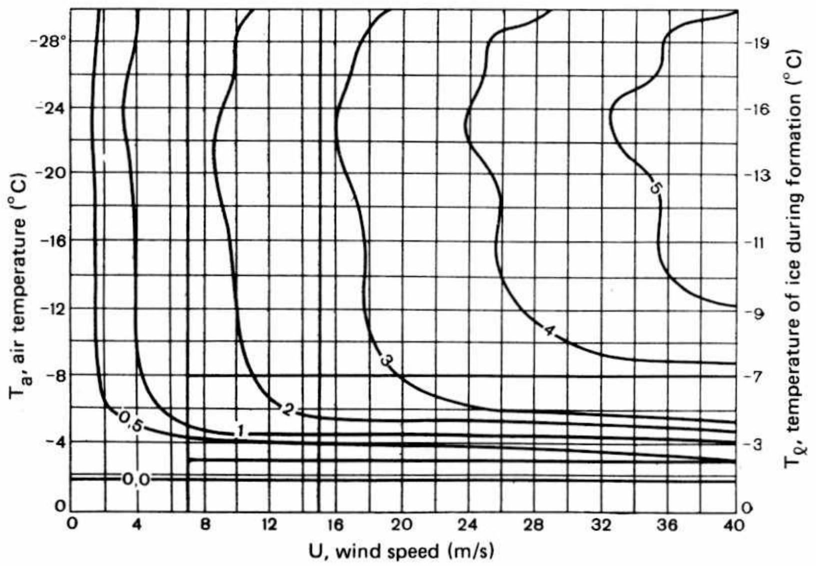

Figure B7. Amount of ice (g/h) which may form on a 1-cm² flat surface during ship icing under the following conditions: $T_w = 1.7°C$, $S = 34\ ^0/_{00}$, $L_z = 4.0$, $L_i = 601 - 686$, $C_\ell = 1.0 - 36.5$, $C_w = 0.96$ (Borisenkov et al. 1971).

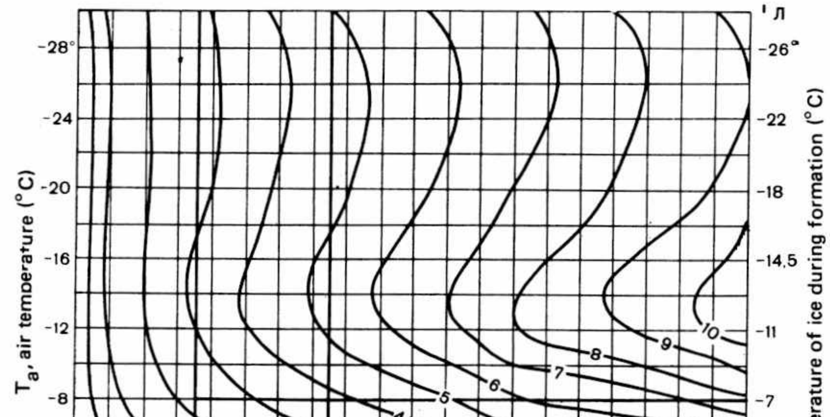

Figure B8. Amount of ice (g/h) which may form on a 1-cm² flat surface during ship icing under the following conditions: $T_w = 2°C$, $S = 34\ ^0/_{00}$, $L_z = 4.0$, $L_i = 601 - 700$, $C_\ell = 0.6 - 36.5$, $C_w = 0.96$ (Borisenkov et al. 1971).

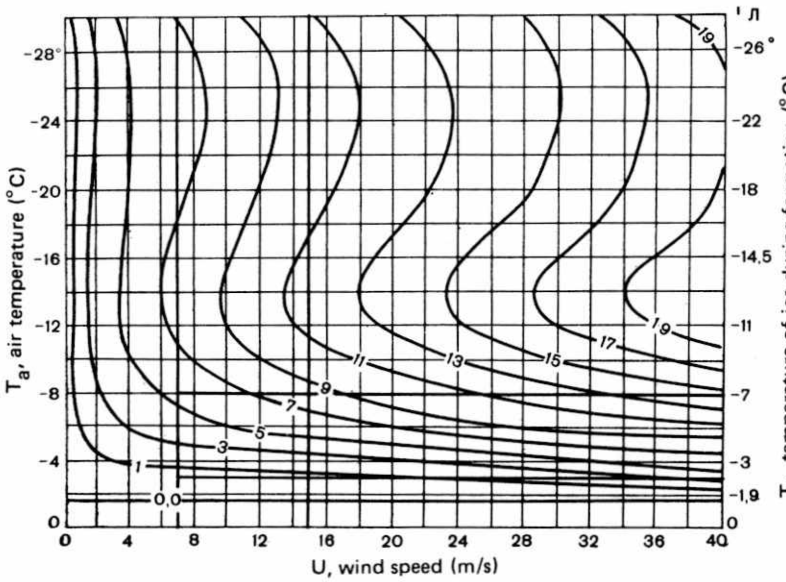

Figure B9. Amount of ice (g/h) which may form on a 1-cm² surface of a 1-cm-diam cylinder during ship icing under the following conditions: $T_w = 2°C$, $S = 34‰$, $L_z = 4.0$, $L_i = 601 - 700$, $C_\ell = 0.6 - 36.5$, $C_w = 0.96$ *(Borisénkov et al. 1971).*

APPENDIX C. ESTIMATION OF ICE ACCUMULATION

An ocean structure can be divided into three zones based on the source of water that will result in icing. Zone 1 is the wave zone that extends to the maximum height of waves. No ice will remain on surfaces in this zone because of flushing action of water across them. Zone 2 is the spray zone that extends to a height of about 50 ft above the peak wave crest. Ice in this zone will result from the spray generated by waves impacting against solid objects in the water, or from spray picked up from wave crests. Zone 3, extending above the spray zone, is the region where only atmospheric sources of water can reach, e.g. wet snow, freezing rain, or supercooled fogs.

Zone 1: Wave zone

In open water, no ice accumulation occurs other than a collar above the fluctuating high water level.

Zone 2: Spray zone

The graphs relating ice growth to wind speed and air temperature will be used. These were derived theoretically by the Russians and applied to practical icing situations with reportedly good correlation (as high as $r = 0.97$). However, design values obtained from these data are subject to verification, particularly since conditions of type of ship or other structure, wind and wave directions, and accreting surface form, attitude, and type will all bear heavily on icing rate. This approach is intended as a first step in obtaining design information.

Case 1. Accreting surface: small cylinder (1 cm diam)
Water source: sea spray (34 ‰ salinity)
Water temperature: 29°F
Wind speed: 24 kt ≈ 12 m/s
Air temperature: 10°F ≈ −12°C.

Use Figure B4. Entering wind speed on abscissa and air temperature on left ordinate, intersection is on curved line 11 g/cm² hr, or 22 lb/ft² hr.

Case 2. We will compare this value with the predicted accumulation rate on a flat surface, all other conditions remaining the same.

Use Figure B5. Intersection of the ordinates is nearly on 5 g/cm² hr ≈ 10 lb/ft² hr, or less than half the small cylinder accretion rate.

As water source temperature rises, accretion rate decreases.

Case 3. Sea water temperature 2°C = 35.6°F
Accreting surface: flat
Water source: sea spray (34 ‰ salinity).

Use Figure B8. Using conditions of cases 1 and 2, I = 4.5 g/cm² hr ≈ 9 lb/ft² hr.

Case 4. Sea water temperature 2°C = 35.6°F
Accreting surface: small cylinder (1 cm diam)
Water source: sea spray (34 ‰ salinity).

Use Figure B9. Using conditions of cases 1 and 2, I = 10 g/cm² hr ≈ 20 lb/ft² hr.

Case 5. Water source: fresh
Accreting surface: flat.

Use Figure B2. Under same conditions as previously stated, I = 0.06 g/cm² hr ≈ 0.12 lb/ft² hr.

IMCO has specified a standard allowance for ice accumulation on fishing vessels: all exposed horizontal surfaces such as decks and gangways are assumed to carry an ice load of 30 kg/m² (6.14 lb/ft²) and the projected vertical area above the waterline (sail area) is assumed to carry an ice load of 15 kg/m² (3.07 lb/ft²). This corresponds to a thickness of 1.4 in. (3.5 cm) for the deck load and half that for the vertical load. These values are very low for many expected icing events, and are in fact exceeded 71% of the time in the Bering Sea and 60% in the Sea of Japan and the Sea of Okhotsk, according to Russian experience, and 80% of the time by German vessels. Japanese researchers recommend design loads of 50 kg/m² (10.2 lb/ft²) for both deck and sail area (Tabata et al. 1963).

Zone 3: Atmospheric zone

In a maritime climate similar to the Gulf of Alaska or the North Sea, icing intensity can be expected to be more severe than in a continental location such as the Moscow region from which the icing data as a function of height were obtained. The general relationship of rime ice and mixture accumulation shown in Figure 7 will likely hold true regardless of location. Therefore, doubling the measured values at the 25-m height is recommended, giving a thickness of about 4 cm in diameter and a mass of 320 g/m. It is questionable whether the extreme glaze accumulation of 4-6 in. (10-15 cm) reported in Great Britain in 1940 would occur offshore; the vertical thermal gradient over water is less extreme than over land, and thus the conditions for development of supercooled rain and for a cold accumulating surface are less likely. A thickness of 5 cm, however, can reasonably be expected.

☆ U. S. GOVT. PRINTING OFFICE 1977 701-548 # 140